Supplementary Information

The Complex Interplay of Chemo- and Bio-catalysis for One-pot Oxidation Cascades – Indole Oxidation in Focus

Alex Stenner[a]*, Richard J. Lewis[a]*, Johnathan Pask[a], David J. Morgan[a,b], Thomas E. Davies[a] and Graham J. Hutchings[a]*

[a]Max Planck–Cardiff Centre on the Fundamentals of Heterogeneous Catalysis FUNCAT, Cardiff Catalysis Institute, School of Chemistry, Cardiff University, CF24 4HQ, United Kingdom.

[b]HarwellXPS, Research Complex at Harwell (RCaH), Didcot, OX11 OFA, United Kingdom.

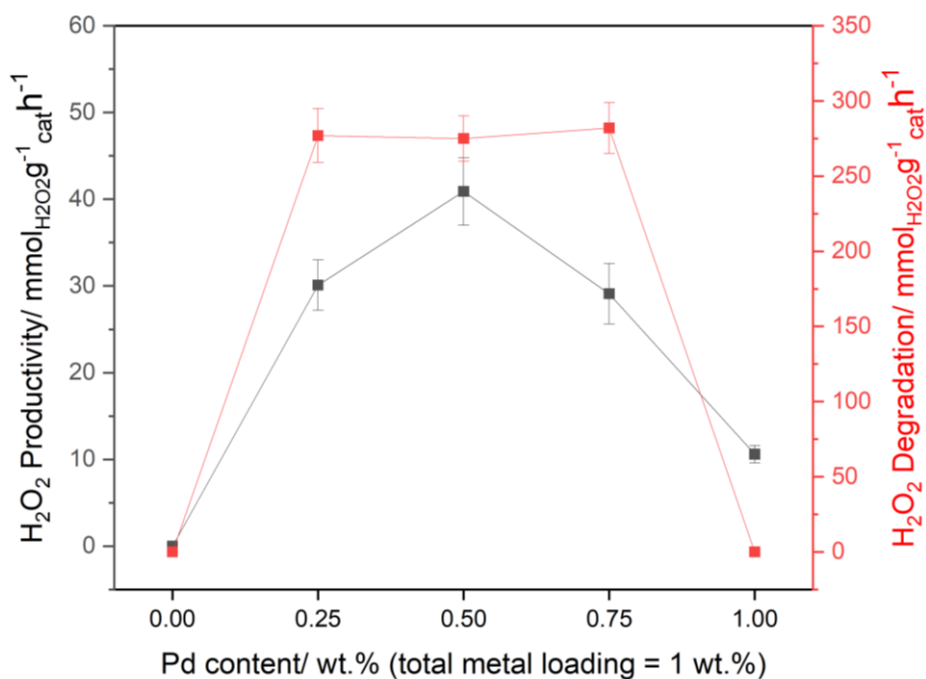*StennerAJ@Cardiff.ac.uk, LewisR27@Cardiff.ac.uk, Hutch@Cardiff.ac.uk

Figure S.1. Catalytic activity of the $1\%Au_xPd_y/TiO_2$ series towards H_2O_2 synthesis and degradation. **H_2O_2 synthesis reaction conditions:** catalyst (0.001 g), 2 bar (80% H_2 in air), potassium phosphate buffer (10 mM, 10 mL, pH 6.0), 250 rpm, 20 °C, 5 minutes. **H_2O_2 degradation reaction conditions:** catalyst (0.001 g), H_2O_2 (2000 ppm), 2 bar (80% H_2 in N_2), potassium phosphate buffer (10 mM, 10 mL, pH 6.0), 250 rpm, 20 °C, 2 h. **Key:** H_2O_2 productivity (*black squares*), H_2O_2 degradation (*red squares*).
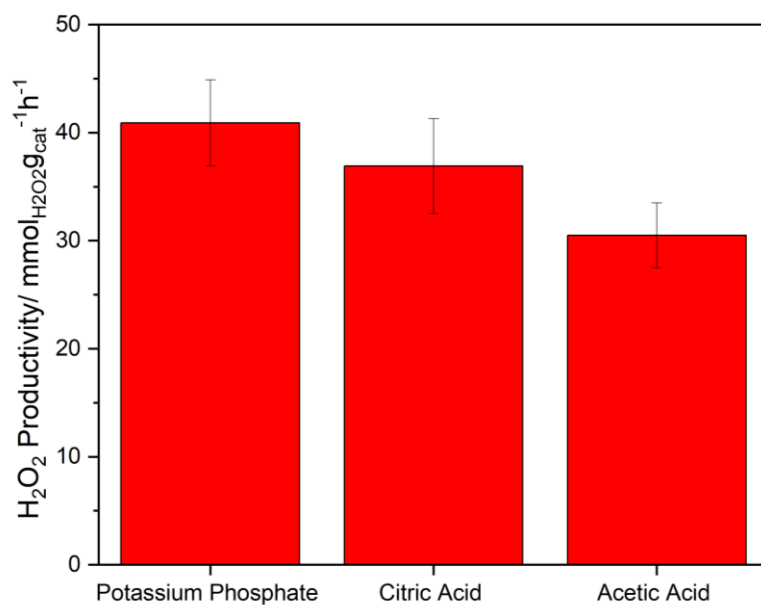
Figure S.2. Catalytic activity of the 1%Au_1Pd_1/TiO_2 formulation towards H_2O_2 synthesis, as a function of solvent buffer. **H_2O_2 synthesis reaction conditions:** catalyst (0.001 g), 2 bar (80% H_2 in air), buffer (10 mL, 100 mM, pH 5.8), 250 rpm, 20 °C, 5 minutes.
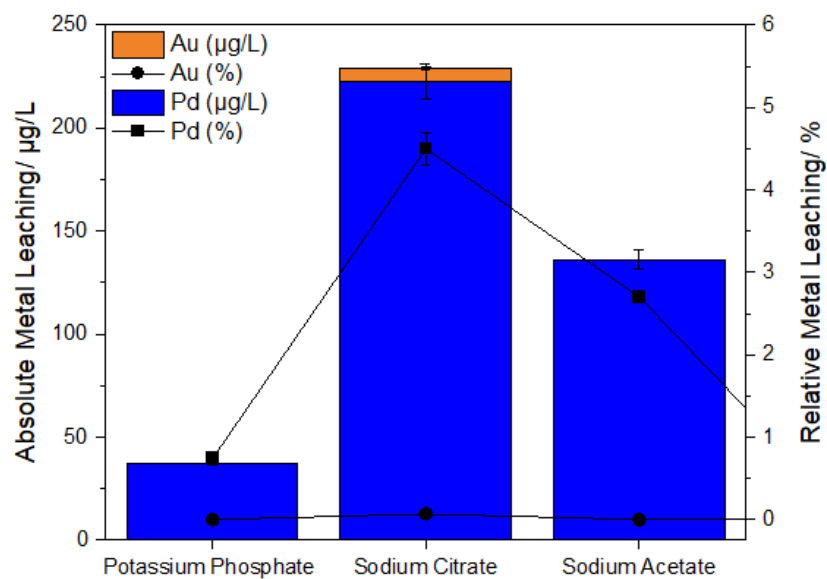
Figure S.3. Extent of metal leaching from the $1\%Au_1Pd_1/TiO_2$ catalyst under model reaction conditions, as a function of buffer selection and determined by ICP-MS of post-reaction solutions. **Model reaction conditions:** catalyst (0.01 g), solvent buffer (10 mL, 100 mM, pH 5.8), 2 bar (80 % H_2 in air), 250 rpm, 20 °C, 2 h.
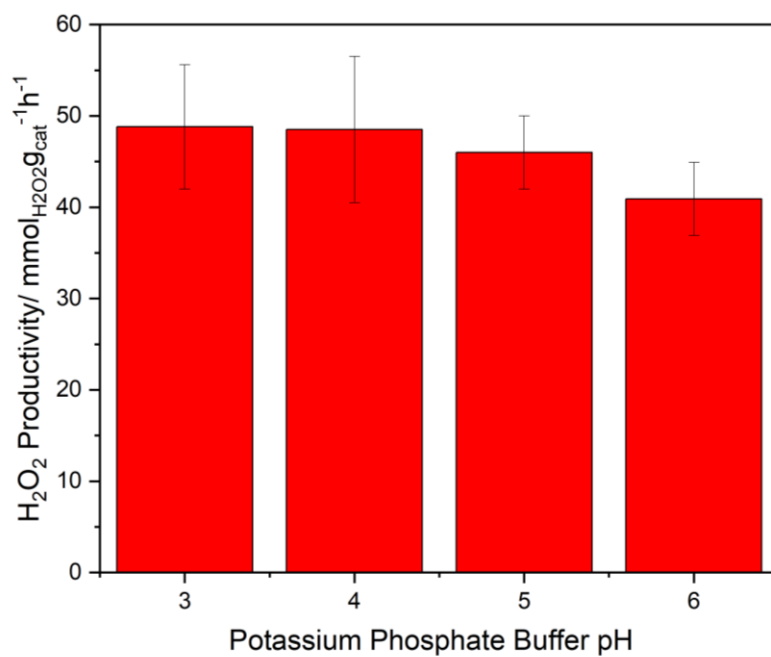
Figure S.4. Catalytic activity of the 1%Au$_1$Pd$_1$/TiO$_2$ formulation towards H$_2$O$_2$ synthesis, as a function of potassium phosphate buffer pH. **H$_2$O$_2$ synthesis reaction conditions:** catalyst (0.001 g), 2 bar (80% H$_2$ in air), potassium phosphate buffer (pH 3.0 – 6.0, 100 mM, 10 mL), 250 rpm 20 °C, 5 minutes.
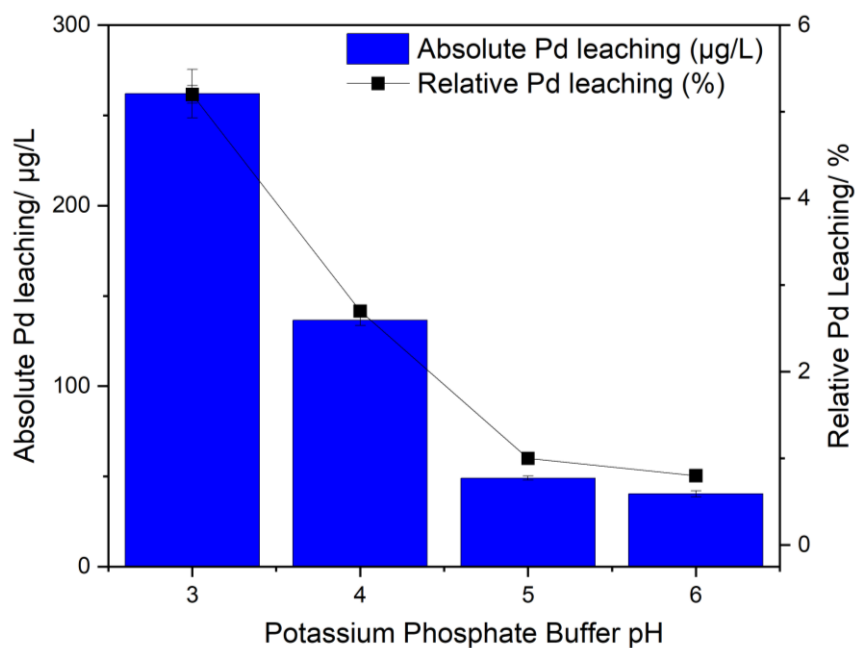
Figure S.5. Extent of metal leaching from the 1%Au$_1$Pd$_1$/TiO$_2$ catalyst into solution under model reaction conditions, as a function of potassium phosphate buffer pH and determined by ICP-MS of post-reaction solutions. **Model Reaction conditions:** catalyst (0.01 g), solvent buffer (pH 3.0 – 6.0, 100 mM, 10 mL), 2 bar (80 % H$_2$ in air), 250 rpm, 20 °C, 2 h. **Note:** Au leaching not observed under reaction conditions.

Figure S.6. Catalytic activity of the 1%Au_1Pd_1/TiO_2 formulation towards H_2O_2 synthesis, as a function of potassium phosphate buffer concentration. **H_2O_2 synthesis reaction conditions:** catalyst (0.001 g), 2 bar (80% H_2 in air), potassium phosphate buffer (10 - 100 mM, 10 mL, pH 5.0), 250 rpm, 20 °C, 5 minutes.

Figure S.7. Extent of metal leaching from 1%Au_1Pd_1/TiO_2 catalyst into solution under model reaction conditions, as a function of potassium phosphate buffer concentration and determined by ICP-MS of post-reaction solutions. **Model reaction conditions:** catalyst (0.01 g), solvent buffer (10 - 100 mM, 10 mL, pH 5.0), 2 bar (80 % H_2 in air), 250 rpm, 20 °C, 2 h. **Note:** Au leaching not observed under reaction conditions.
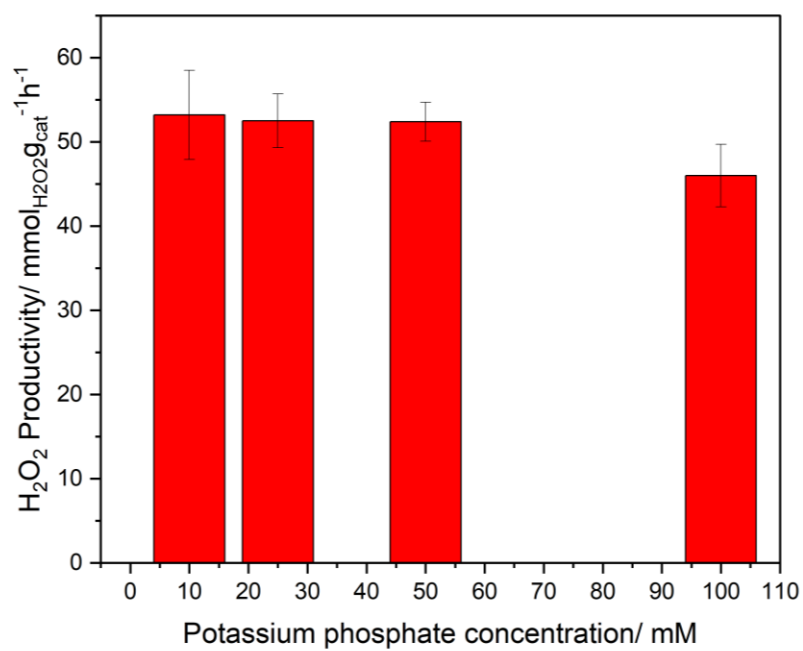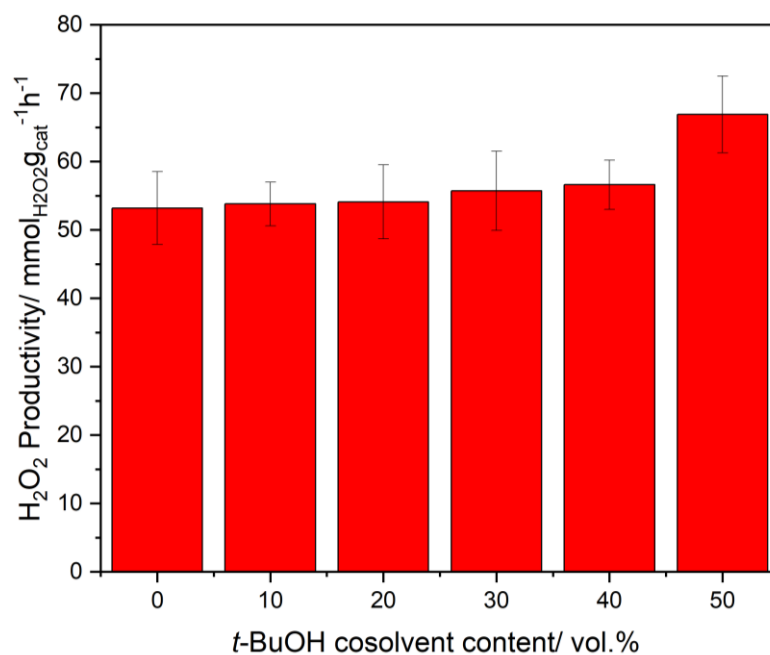
Figure S.8. Catalytic activity of 1%Au$_1$Pd$_1$/TiO$_2$ formulation towards the initial rate of H$_2$O$_2$ synthesis, as a function of t-BuOH content. **H$_2$O$_2$ synthesis reaction conditions:** catalyst (0.001 g), 2 bar (80% H$_2$ in air), potassium phosphate buffer (10 mM, 5 - 10 mL, pH 5.0), t-BuOH (0 – 50 vol.%), 250 rpm, 20 °C, 5 minutes.
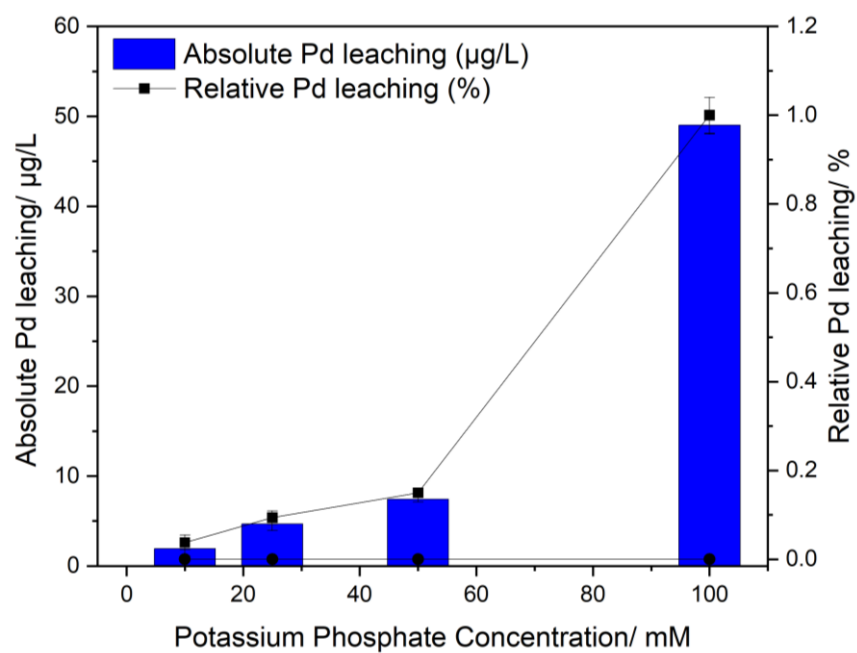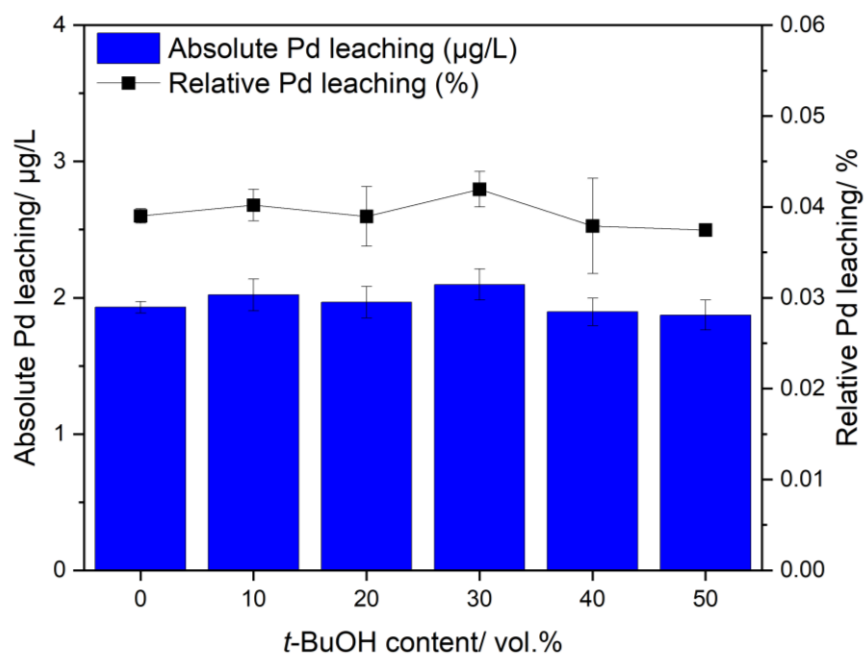
Figure S.9. Extent of metal leaching from 1%Au$_1$Pd$_1$/TiO$_2$ catalyst into solution under model reaction conditions, as a function of t-BuOH content and determined by ICP-MS of post-reaction solutions. **Model reaction conditions:** catalyst (0.01 g), potassium phosphate buffer (5 – 10 mL, 10 mM, pH 5.0), t-BuOH (0 – 50 vol.%), 2 bar (80 % H$_2$ in air), 250 rpm, 20 °C, 2 h. **Note:** Au leaching not observed.
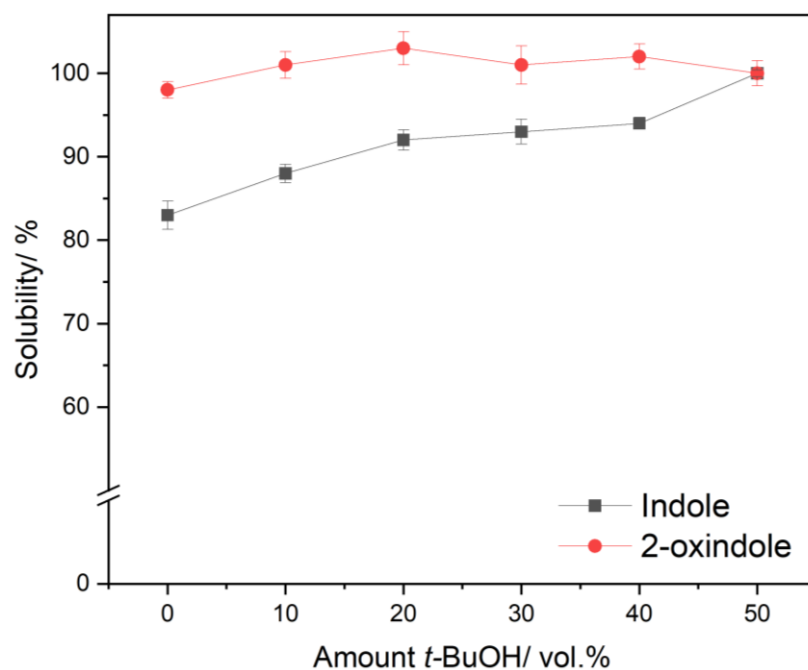
Figure S.10. Solubility of indole and 2-oxindole in *t*-BuOH/potassium phosphate buffer mixtures. **Reaction conditions:** indole or 2-oxindole (10 mM), potassium phosphate buffer (5 – 10 mL, 10 mM, pH 5.0) with *t*-BuOH (0 – 50 vol.%), 500 rpm, 0.5 h.

Table S.1. Catalytic activity of the 1%$Au_x$$Pd_y$/$TiO_2$ series towards the H_2O_2 direct synthesis, under previously established and modified reaction conditions.

Catalyst	Previously Established Reaction Conditions		Modified Reaction Conditions	
	Rate/ $mmol_{H2O2}g_{cat}^{-1}h^{-1}$	TOF/ $mmol_{H2O2}mmol_{metal}^{-1}h^{-1}$	Rate/ $mmol_{H2O2}g_{cat}^{-1}h^{-1}$	TOF/ $mmol_{H2O2}mmol_{metal}^{-1}h^{-1}$
1% Au/TiO_2	0.0 ± 0.0	0.0 ± 0.0	3.1 ± 1	60.4 ± 12
1% Au_3Pd_1/TiO_2	30.1 ± 2.9	489 ± 47	62.7 ± 7.1	1019 ± 116
1% Au_1Pd_1/TiO_2	40.9 ± 3.9	565 ± 54	66.8 ± 5.6	923 ± 77
1% Au_1Pd_3/TiO_2	29.1 ± 3.5	350 ± 42	56.8 ± 5.6	683 ± 68
1% Pd/TiO_2	10.6 ± 1.0	112 ± 2.0	23.7 ± 3.8	252 ± 40

Previously established H_2O_2 synthesis reaction conditions: catalyst (0.001 g), 2 bar (80% H_2 in air), potassium phosphate buffer (100 mM, pH 6.0, 10 mL), 250 rpm, 20 °C, 5 minutes. **Modified H_2O_2 synthesis reaction conditions:** catalyst (0.001 g), 2 bar (80% H_2 in air), potassium phosphate buffer (10 mM, pH 5.0, 10 mL) with 50 vol.% *t*-BuOH, 250 rpm, 20 °C, 5 minutes.

Table S.2. Extent of metal leaching from the 1%Au_xPd_y/TiO_2 catalyst series under model H_2O_2 synthesis reaction conditions, as determined *via* ICP-MS of post-reaction solutions.

Catalyst	Extent of Pd Leaching			
	Previously Established Reaction Conditions		Modified Reaction Conditions	
	Leaching/ ug$_{Pd}$/L	Leaching / %	Leaching/ ug$_{Pd}$/L	Leaching / %
1% Au/TiO_2	0.0	0.0	0.0	0.0
1% Au_3Pd_1/TiO_2	10.4 ± 0.52	0.42 ± 0.01	2.9 ± 0.52	0.11 ± 0.02
1% Au_1Pd_1/TiO_2	40.4 ± 0.32	0.82 ± 0.03	6.9 ± 0.32	0.01 ± 0.01
1% Au_1Pd_3/TiO_2	48.7 ± 1.00	0.63 ± 0.01	5.2 ± 1.00	0.07 ± 0.01
1% Pd/TiO_2	59.1 ± 1.07	0.59 ± 0.01	7.5 ± 1.07	0.07 ± 0.01

Previously established H_2O_2 synthesis reaction conditions: catalyst (0.01 g), 2 bar (80% H_2 in air), potassium phosphate buffer (100 mM, 10 mL, pH 6.0), 250 rpm 20 °C, 2 h. **Modified H_2O_2 synthesis reaction conditions:** catalyst (0.01 g), 2 bar (80% H_2 in air), potassium phosphate buffer (10 mM, 10 mL, pH 5.0) with 50 vol.% *t*-BuOH, 250 rpm 20 °C, 2 h. **Note 1:** ten-times the typical catalyst mass (0.01 g) employed to allow accurate determination of leached metal species by ICP-MS. **Note 2:** Au leaching not observed.
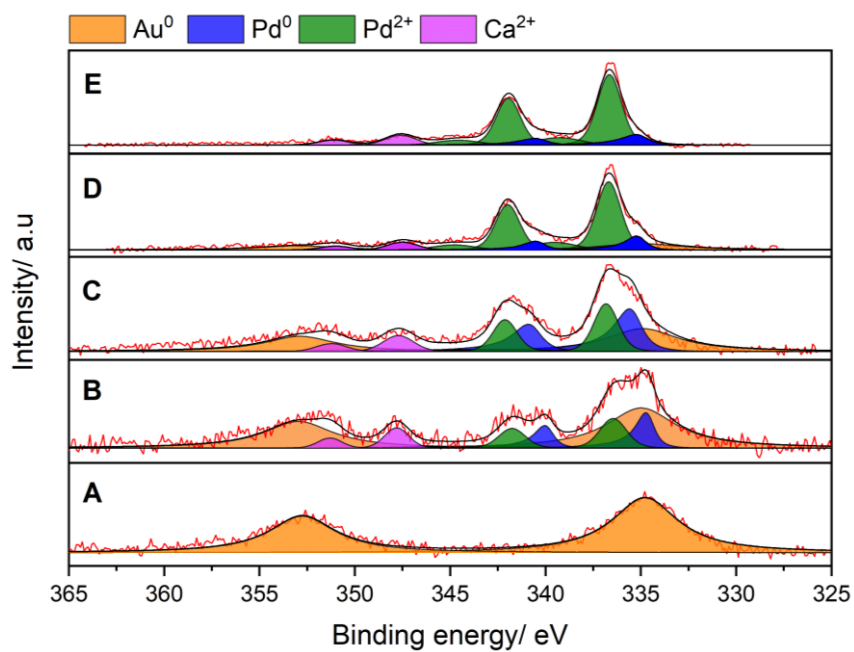
Figure S.11. XPS analysis showing the surface atomic compositions in the Pd (3d) region of the as-prepared 1%Au$_x$Pd$_y$/TiO$_2$ catalyst series prepared by sol-immobilization. **Key: A)** 1%Au/TiO$_2$, **B)** 1%Au$_3$Pd$_1$/TiO$_2$, and **C)** 1%Au$_1$Pd$_1$/TiO$_2$ **D)** 1%Au$_1$Pd$_3$/TiO$_2$, **E)** 1%Pd/TiO$_2$.

Table S.3. Summary of the surface atomic composition of Pd 3d region of the as-prepared the $1\%Au_xPd_y/TiO_2$ catalyst series, as determined by XPS, corresponding to the spectra shown in Figure S.11.

Catalyst	Pd: Au	$Pd^{2+}: Pd^0$
1% Au/TiO_2	-	-
1% Au_3Pd_1/TiO_2	1: 1.5	1: 1.7
1% Au_1Pd_1/TiO_2	1: 0.4	1: 1.6
1% Au_1Pd_3/TiO_2	1: 0.1	1: 0.2
1% Pd/TiO_2	-	1: 0.3

Table S.4. Comparison of H_2O_2 synthesis steady state activity over the 1%Au_xPd_y/TiO_2 catalyst series, determined at 3 h reaction time.

Catalyst	H_2O_2 Direct Synthesis Steady State Activity/ $mol_{H2O2}g_{cat}^{-1}h^{-1}$
1% Au/TiO_2	0.4 ± 0.1
1% Au_3Pd_1/TiO_2	2.7 ± 0.3
1% Au_1Pd_1/TiO_2	1.6 ± 0.4
1% Au_1Pd_3/TiO_2	2.8 ± 0.4
1% Pd/TiO_2	6.3 ± 0.3

H_2O_2 direct synthesis reaction conditions: catalyst (0.001 g), 2 bar (80% H_2 in air), potassium phosphate buffer (10 mM, pH 5.0, 10 mL) with 50 vol.% *t*-BuOH, 250 rpm, 20 °C, 3 h.
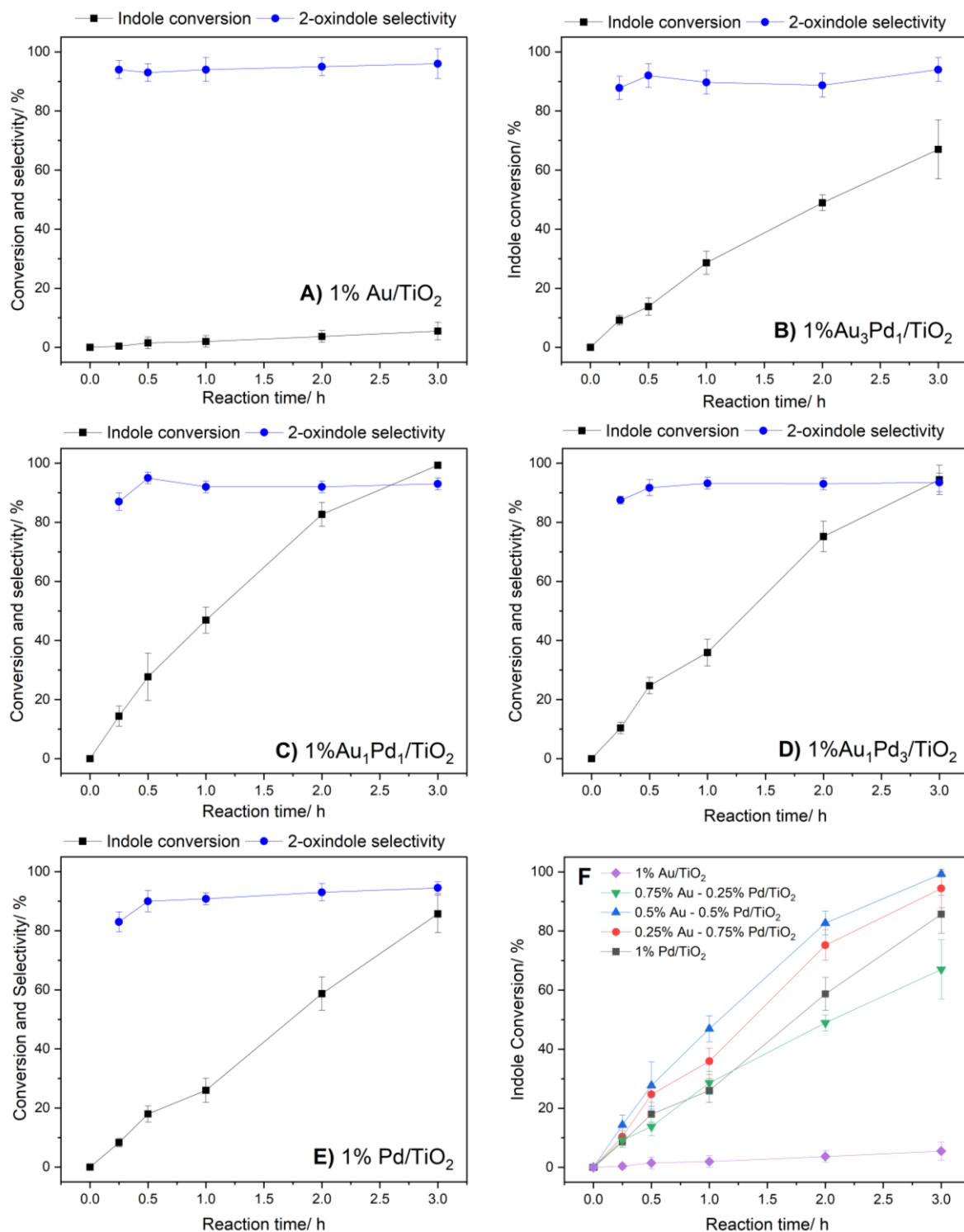
Figure S.12. Catalytic activity of the 1%Au$_x$Pd$_y$/TiO$_2$ catalyst series towards indole oxidation in the CPO chemo-enzymatic cascade, as a function of catalyst formulation. **Indole oxidation reaction conditions:** catalyst (0.001 g), CPO (600 nM, 15 UmL^{-1}), indole (10 mM), potassium phosphate buffer (10 mM, 10 mL, pH 5.0) with 50 vol.% t-BuOH, 2 bar (80 % H$_2$ in air), 250 rpm, 20 °C, 0 – 3 h.
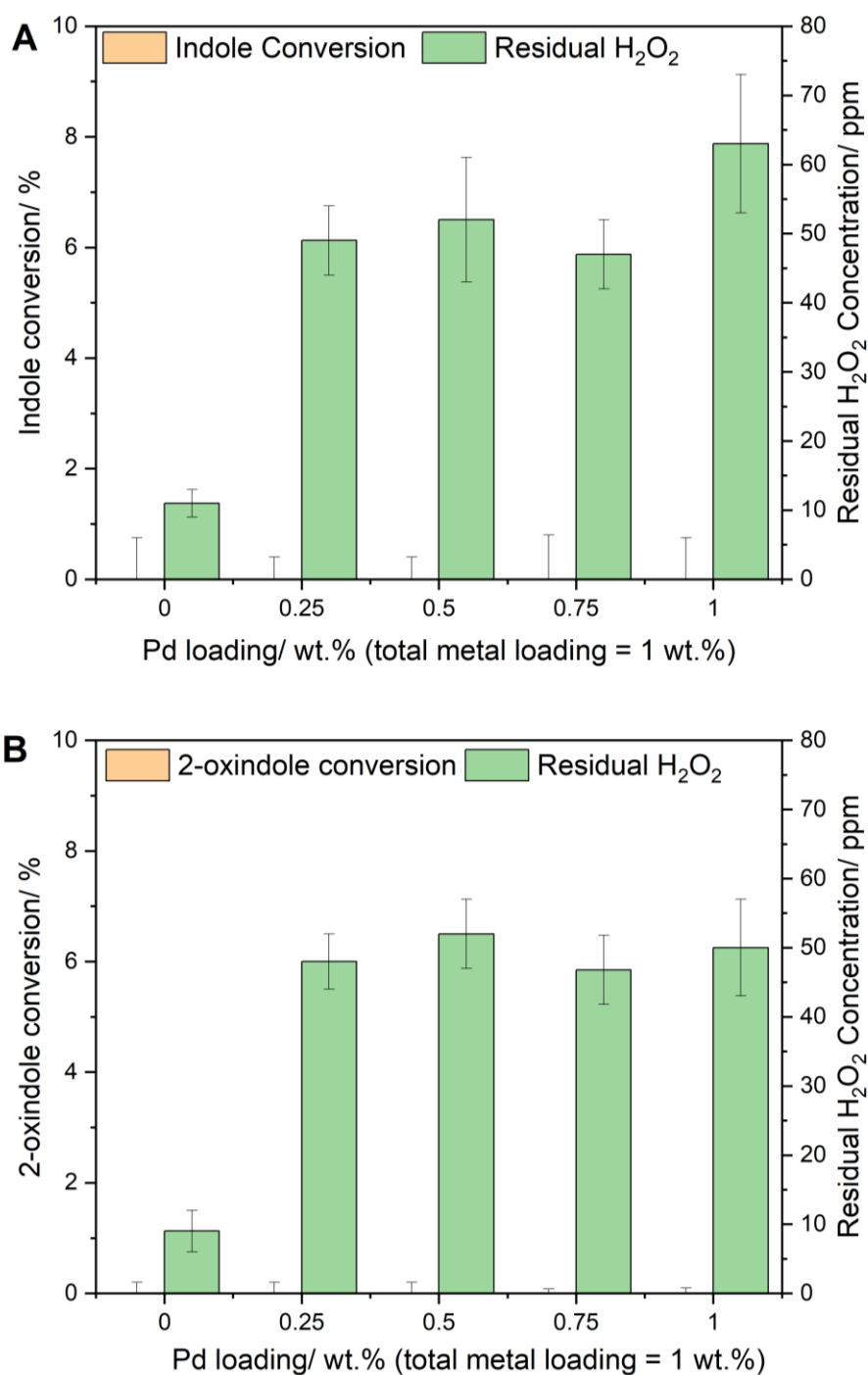
Figure S.13. Chemo-catalytic activity towards **A)** indole and **B)** 2-oxindole, in the absence of CPO. **Chemo-catalytic indole/2-oxindole reaction conditions:** catalyst (0.001 g), indole or 2-oxindole (10 mM), potassium phosphate buffer (10 mM, 10 mL, pH 5.0) with 50 vol.% *t*-BuOH, 2 bar (80 % H_2 in air), 250 rpm, 20 °C, 2 h.

Figure S.14. Comparison of enzymatic (with *in situ* and *ex situ* supplied H_2O_2) and chemo-catalytic only (1%Au_xPd_y/TiO_2 series) activity towards 2-oxindole. **A) *in situ* supplied oxidant reaction conditions:** 1%Au_1Pd_1/TiO_2 (0.001 g), CPO (600 nM, 15 UmL^{-1}), 2-oxindole (10 mM), potassium phosphate buffer (10 mM, 10 mL, pH 5.0) with 50 vol.% *t*-BuOH, 2 bar (80 % H_2 in air), 250 rpm, 20 °C, 2 h. **B) *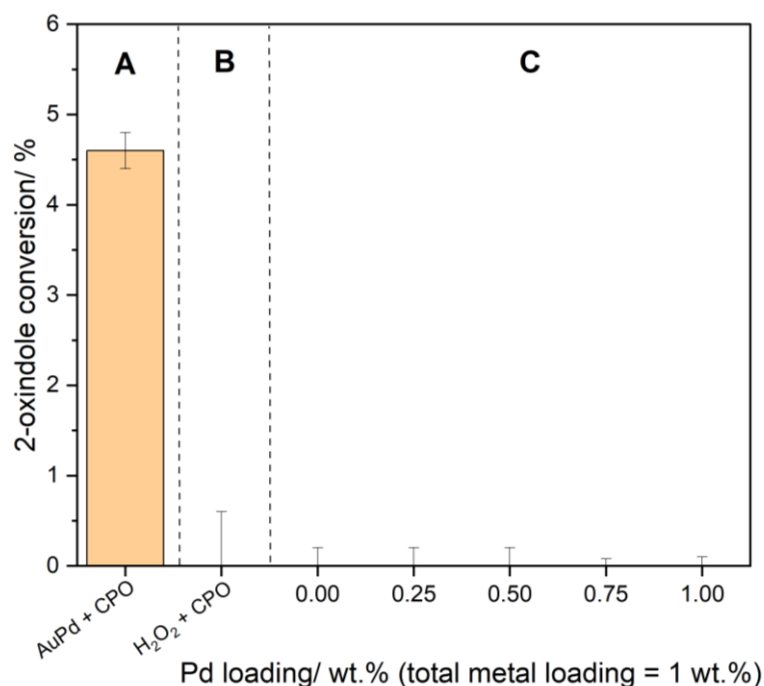ex situ* supplied oxidant reaction conditions:** H_2O_2 (100 ppm), CPO (600 nM, 15 UmL^{-1}), 2-oxindole (10 mM), potassium phosphate buffer (10 mM, 10 mL, pH 5.0) with 50 vol.% *t*-BuOH, 2 bar N_2, 250 rpm, 20 °C, 2 h. **C) chemo-catalytic reaction conditions:** catalyst (0.001 g), 2-oxindole (10 mM), potassium phosphate buffer with (10 mM, 10 mL, pH 5.0) 50 vol.% *t*-BuOH, 2 bar (80 % H_2 in air), 250 rpm, 20 °C, 2 h.

Table S5: Extent of chemo-catalytic activity towards indole under H_2-only reaction conditions, as a function of catalyst formulation.

Catalyst	Indole hydrogenation/ %
1% Au/TiO$_2$	0 ± 0.6
1% Au$_3$Pd$_1$/TiO$_2$	0 ± 0.4
1% Au$_1$Pd$_1$/TiO$_2$	0 ± 0.8
1% Au$_1$Pd$_3$/TiO$_2$	0 ± 0.7
1% Pd/TiO$_2$	0 ± 0.6

Reaction conditions: catalyst (0.001 g), indole (10 mM), potassium phosphate buffer (10 mM, 10 mL, pH 5.0) with 50 vol.% *t*-BuOH, 2 bar (80 % H_2 in N_2), 250 rpm, 20 °C, 2 h.

Table S.6. Comparison of catalytic activity towards indole oxidation, as an effect of oxidant.

Reaction Conditions	Indole Conversion/ %
CPO + 1% Au_1Pd_1/TiO_2 + H_2 + O_2	82.7 ± 4.0
CPO + 0.5%Pd/TiO_2 + H_2 + O_2	32.8 ± 2.6
CPO + TiO_2 + H_2 + O_2	0.0 ± 0.0
CPO + 1% Au_1Pd_1/TiO_2 + O_2 (N_2)	0.0 ± 0.0
CPO + 1% Au_1Pd_1/TiO_2 + H_2 (N_2)	1.6 ± 1.1
CPO + O_2*	0.0 ± 0.0

Indole oxidation reaction conditions: catalyst (0.001 g), CPO (600 nM, 15 UmL^{-1}), indole (10 mM), potassium phosphate buffer with 50 vol.% t-BuOH (10 mM, 10 mL, pH 5.0), 2 bar (80 % H_2 in air), 250 rpm, 20 °C, 2 h. **Note:** (N_2) indicates pressure maintained with N_2 in place of O_2 (as air) or H_2, as indicated. *Reaction conducted at ambient pressure in sealed vessel.

Table S.7. Effect of *in situ* and *ex situ* oxidant supply on the rate of CPO deactivation.

H_2O_2 Supply	Conversion/ %	Substrate converted (mol)/ CPO deactivated (mol)
1% Au_1Pd_1/TiO_2	14	16,840
	83	31,050
0.7 mM H_2O_2	6	6,730
1.5 mM H_2O_2	9	10,100
2.9 mM H_2O_2	14	11,800
10 mM H_2O_2	16	9,000

Chemo-enzymatic indole oxidation reaction conditions: catalyst (0.001 g), CPO (600 nM, 15 UmL^{-1}), indole (10 mM), potassium phosphate buffer (10 mM, 10 mL, pH 5.0) with 50 vol.% *t*-BuOH, 2 bar (80 % H_2 in air), 250 rpm, 20 °C, 2 h. **Indole oxidation with pre-formed H_2O_2:** H_2O_2 (0.7 – 10 mM, 25 – 340 ppm), CPO (600 nM, 15 UmL^{-1}), indole (10 mM), potassium phosphate buffer (10 mM, 10 mL, pH 5.0) with 50 vol.% *t*-BuOH, 2 bar (80 % H_2 in air), 250 rpm, 20 °C, 2 h. **Note:** pre-formed H_2O_2 was added in a single injection to initiate the reaction.
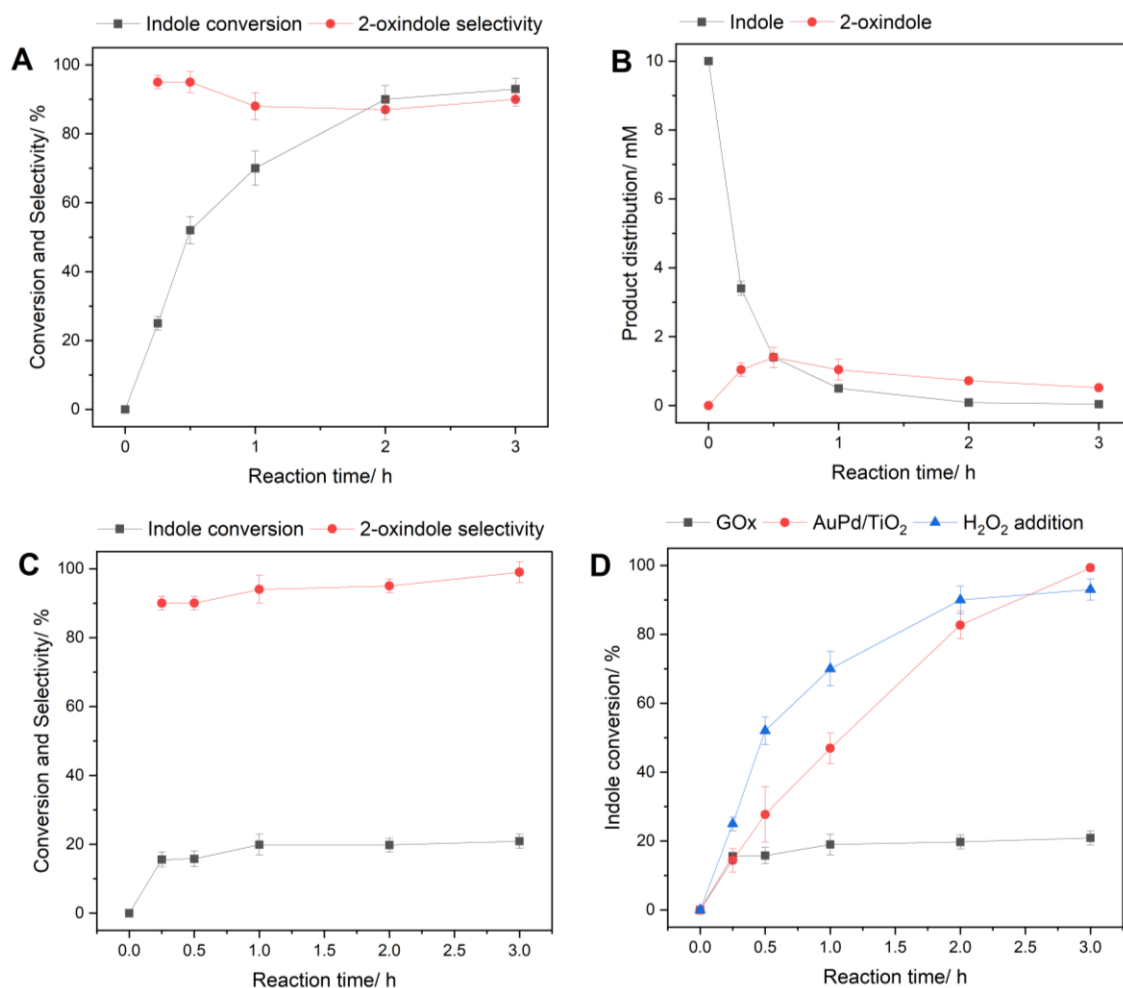
Figure S.15. Comparison of enzymatic performance towards indole oxidation, as a function of H_2O_2 supply strategy. **Continuous oxidant addition reaction conditions (A, B, D):** H_2O_2 (1.36 mM), pump (50 mL/h), CPO (15 UmL^{-1}, 600 nM), indole (10 mM), potassium phosphate buffer (10 mL, 10 mM, pH 5.0) with 50 vol.% t-BuOH, ambient pressure, 250 rpm, 20 °C, 0 – 3 h. **Co-enzymatic reaction conditions (C, D):** glucose oxidase (0.2 U/mL), glucose (100 mM), CPO (15 UmL^{-1}, 600 nM), indole (10 mM), potassium phosphate buffer (10 mL, 10 mM, pH 5.0) with 50 vol.% t-BuOH, ambient pressure, 250 rpm, 20 °C, 0 – 3 h. **Chemo-enzymatic reaction conditions (D):** 1%Au$_1$Pd$_1$/TiO$_2$ (0.001), CPO (15 UmL^{-1}, 600 nM), indole (10 mM), potassium phosphate buffer (10 mL, 10 mM, pH 5.0) with 50 vol.% t-BuOH, 2 bar (80% H_2 in air), ambient pressure, 250 rpm, 20 °C, 0 – 3 h.
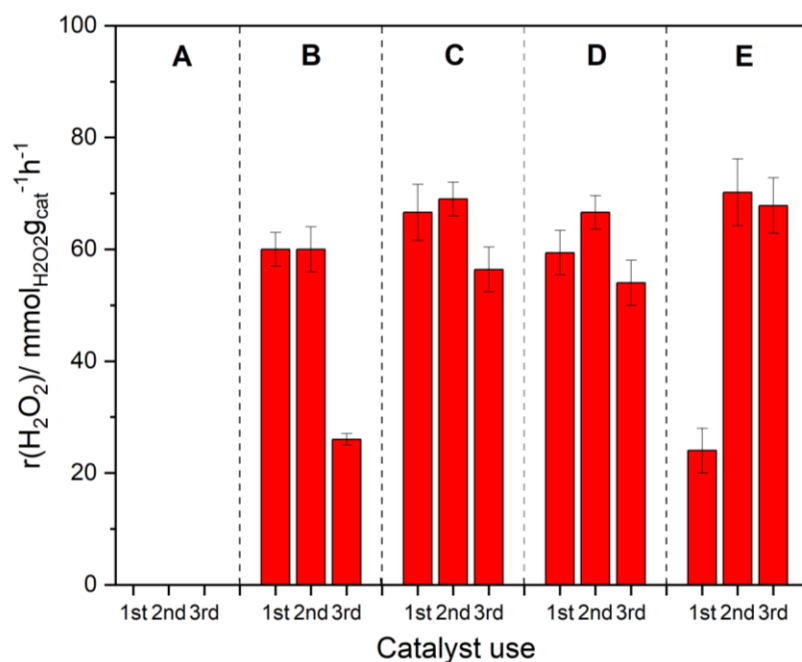
Figure S.16. Catalytic activity of the 1%AuPd/TiO$_2$ series towards H$_2$O$_2$ synthesis, as a function of catalytic reuse. **H$_2$O$_2$ synthesis reaction conditions:** catalyst (0.001 g), 2 bar (80% H$_2$ in air), potassium phosphate buffer (10 mM, pH 5.00, 10 mL) with 50 vol.% *t*-BuOH, 250 rpm, 20 °C, 5 minutes. **Generation of used catalysts:** catalyst (0.01 g), 2 bar (80% H$_2$ in air), potassium phosphate buffer (10 mM, pH 5.0, 10 mL) with 50 vol.% t-BuOH, 250 rpm, 20 °C, 2 h. **Key: A)** 1%Au/TiO$_2$, **B)** 1%Au$_3$Pd$_1$/TiO$_2$, **C)** 1%Au$_1$Pd$_1$/TiO$_2$, **D)** 1%Au$_1$Pd$_1$/TiO$_2$, and **E)** 1%Pd/TiO$_2$.
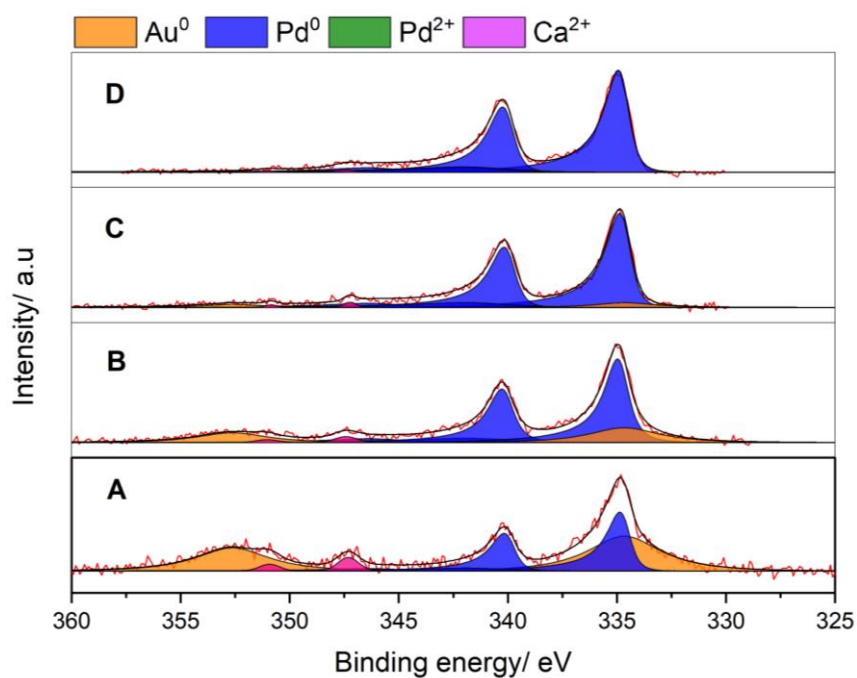
Figure S17. XPS analysis showing the surface atomic compositions in the Pd (3d) region of the Pd-containing catalysts after use in the H_2O_2 synthesis reaction. **Model H_2O_2 synthesis reaction conditions:** catalyst (0.01 g), 2 bar (80% H_2 in air), potassium phosphate buffer (10 mM, pH 5.0, 10 mL) with 50 vol.% t-BuOH, 250 rpm, 20 °C, 2 h. **Key: A)** 1%Au_3Pd_1/TiO_2, **B)** 1%Au_1Pd_1/TiO_2 **C)** 1%Au_1Pd_3/TiO_2, and **D)** 1%Pd/TiO_2.
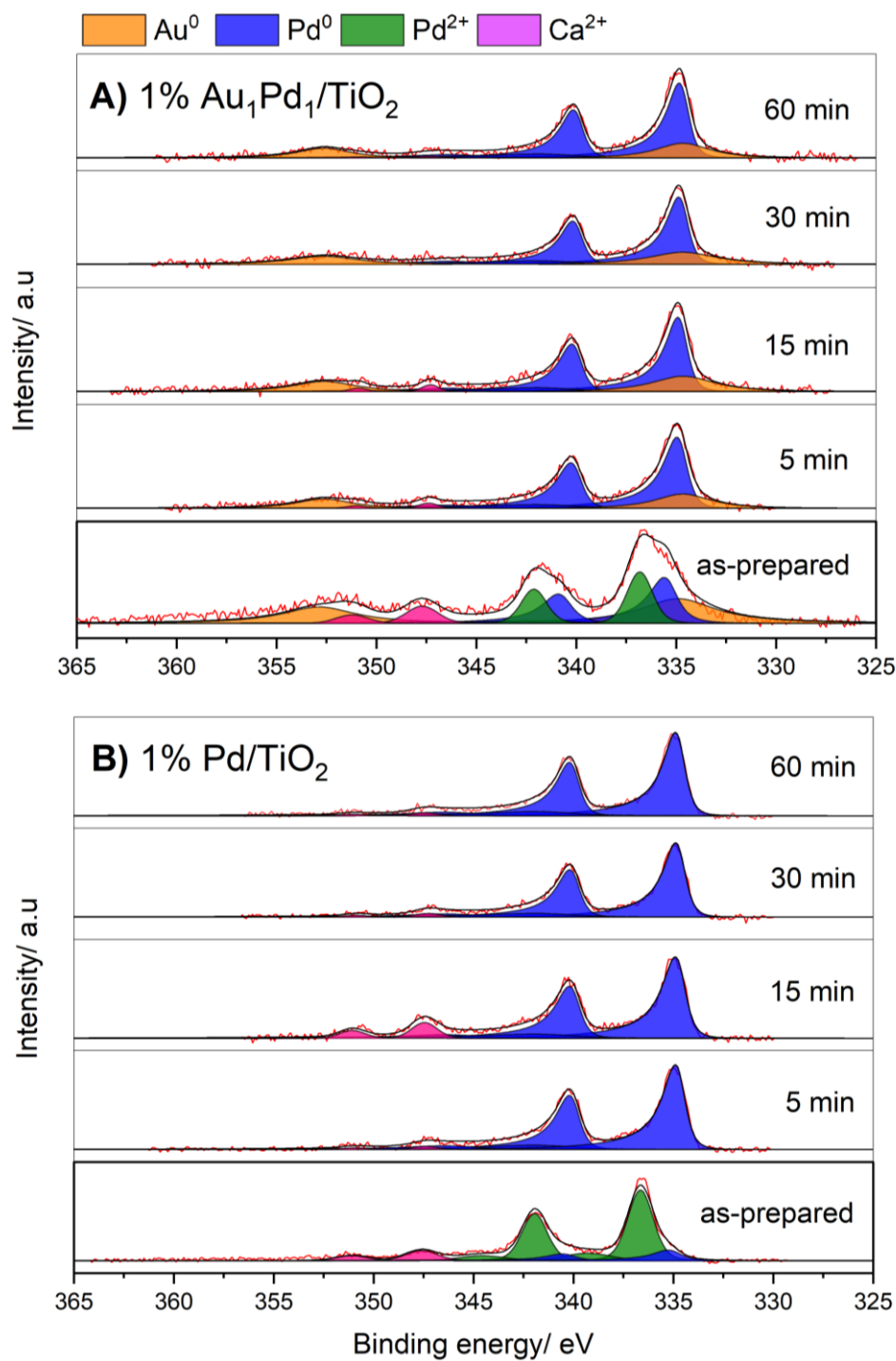
Figure S.18. XPS analysis showing the surface atomic compositions in the Pd (3d) region of the **A)** 1% Au$_1$Pd$_1$/TiO$_2$ and **B)** 1% Pd/TiO$_2$, as a function of reaction time. **Model H$_2$O$_2$ synthesis reaction conditions:** catalyst (0.01 g), 2 bar (80% H$_2$ in air), potassium phosphate buffer (10 mM, pH 5.0, 10 mL) with 50 vol.% t-BuOH, 250 rpm, 20 °C, 5 – 60 minutes.
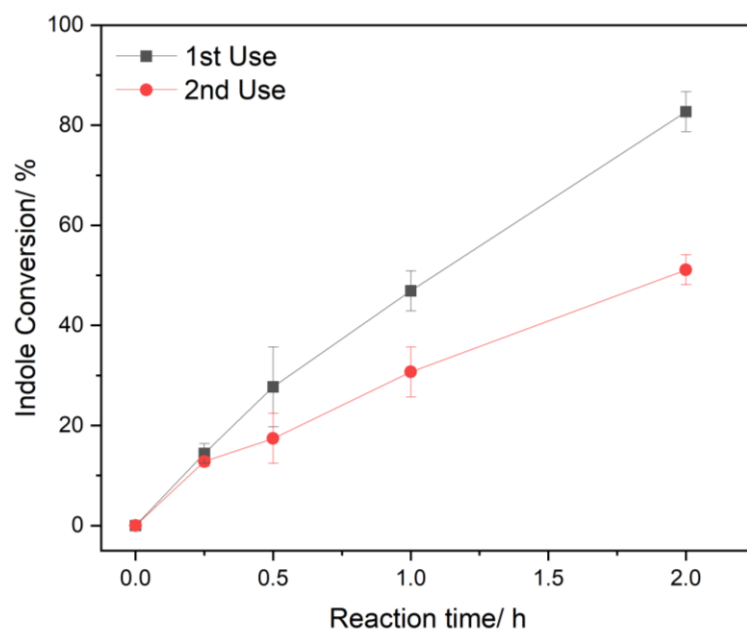
Figure S.19. Effect of chemo-catalyst reuse on the chemo-enzymatic cascade efficacy towards indole oxidation. **Indole oxidation reaction conditions:** catalyst (0.001 g), CPO (600 nM, 15 UmL^{-1}), indole (10 mM), potassium phosphate buffer (10 mM, 10 mL, pH 5.0) with 50 vol.% *t*-BuOH, 2 bar (80 % H$_2$ in air), 250 rpm, 20 °C, 0 – 3 h. **Generation of used catalyst:** catalyst (0.01 g), potassium phosphate buffer (10 mM, 10 mL, pH 5.0) with 50 vol.% *t*-BuOH, 2 bar (80 % H$_2$ in air), 250 rpm, 20 °C, 2 h.

Figure S.20. Effect of chemo-catalyst reuse on H_2O_2 synthesis, as a function of reaction time. **H_2O_2 synthesis reaction conditions:** catalyst (0.001 g), potassium phosphate buffer (10 mL, 10 mM, pH 5.0) with 50 vol.% t-BuOH, 2 bar (80 % H_2 in air), 250 rpm, 20 °C, 0 – 2 h. **Generation of used catalyst:** catalyst (0.01 g), potassium phosphate buffer (10 mM, 10 mL, pH 5.0) with 50 vol.% t-BuOH, 2 bar (80 % H_2 in air), 250 rpm, 20 °C, 2 h.
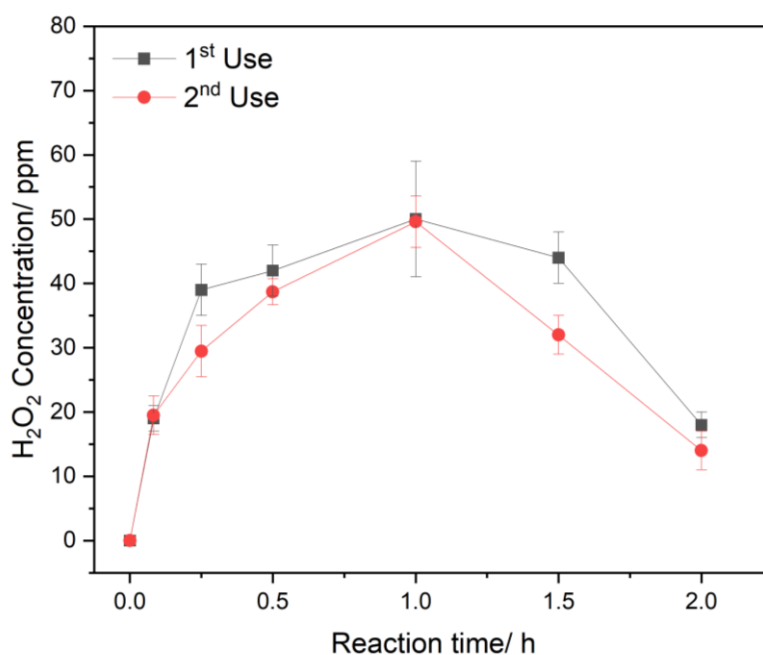
Table S8. Extent of metal leaching from the $1\%Au_1Pd_1/TiO_2$ catalyst over multiple uses, as determined by ICP-MS.

Catalyst	Use	Pd leaching/ µg/L	Pd leaching/ %
$1\%Au_1Pd_1/TiO_2$	1st	6.9 ± 1	0.14 ± 0.03
	2nd	35 ± 0.5	0.69 ± 0.01

Reaction conditions: catalyst (0.01 g), 2 bar (80% H_2 in air), potassium phosphate buffer (10 mM, pH 5.0, 10 mL) with 50 vol.% t-BuOH, 250 rpm, 20 °C, 2 h. **Generation of used catalyst**: catalyst (0.01 g), potassium phosphate buffer (10 mM, pH 5.0, 10 mL) with 50 vol.% t-BuOH, 2 bar 80 % H_2 in air, 250 rpm, 20 °C, 2 h. **Note:** ten-times the typical catalyst mass (0.01 g) employed to allow accurate determination of leached metal species by ICP-MS.
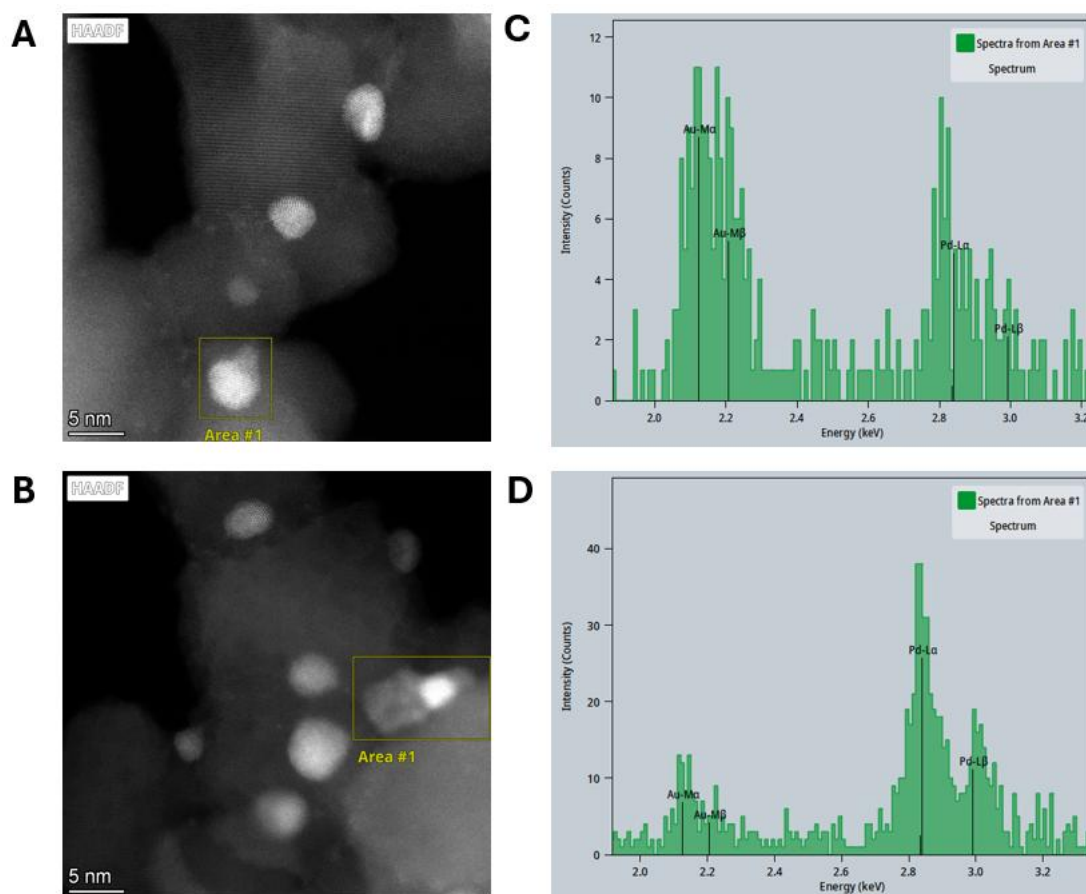
Figure S.21. A-B) HAADF AC-STEM images of the as-prepared 1%Au_1Pd_1/TiO_2 and **(C-D)** corresponding X-EDS spot analysis revealing AuPd nanoalloy particles.

Figure S.22. Particle size distribution of the as-prepared 1% Au_1Pd_1/TiO_2 formulation, as determined *via* AC-STEM imaging. **Note:** Particle counting conducted with *NanoDetect* software.

Figure S.23. HAADF AC-STEM image of the as-prepared 1% Au_1Pd_1/TiO_2 with X-EDS spot analysis revealing the presence of sub-nano (< 1 nm) monometallic Pd species.

Figure S.24. A-B) HAADF AC-STEM images of the used 1%Au_1Pd_1/TiO_2 and **(C-D)** corresponding X-EDS spot analysis revealing the presence of large AuPd nanoalloy particles and aggregates.
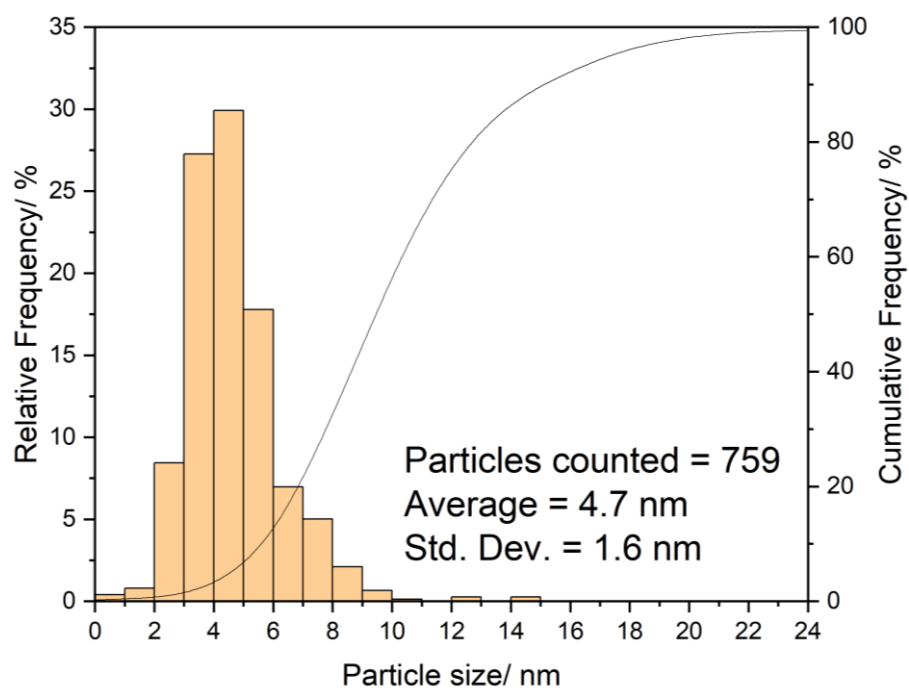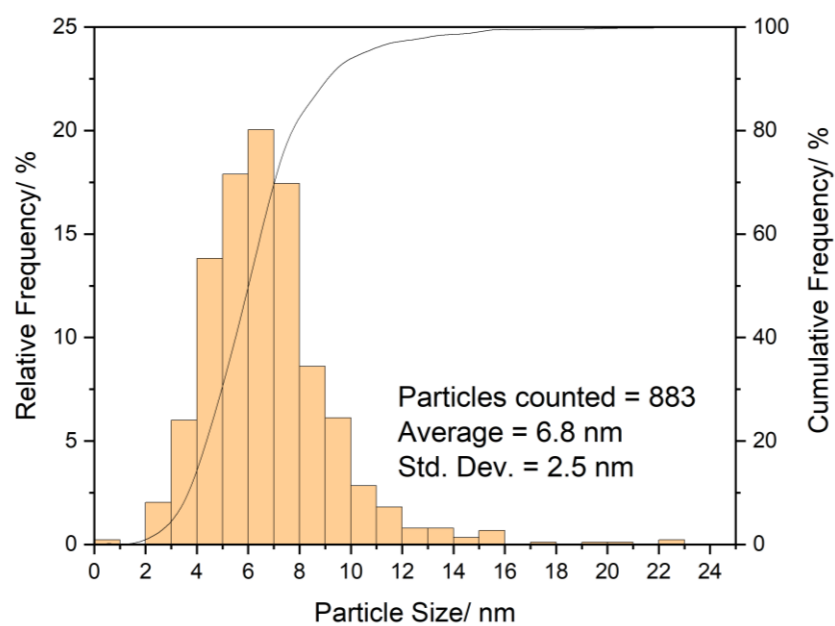
Figure S.25. Particle size distribution of the used 1% Au_1Pd_1/TiO_2 formulation, as determined *via* AC-STEM imaging. **Note:** Particle counting conducted with *NanoDetect* software.
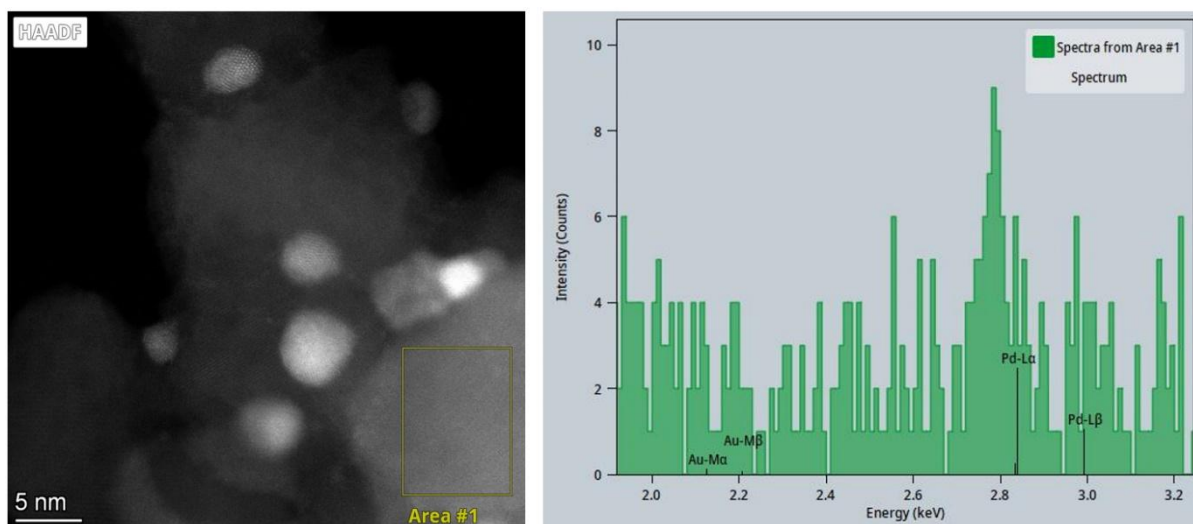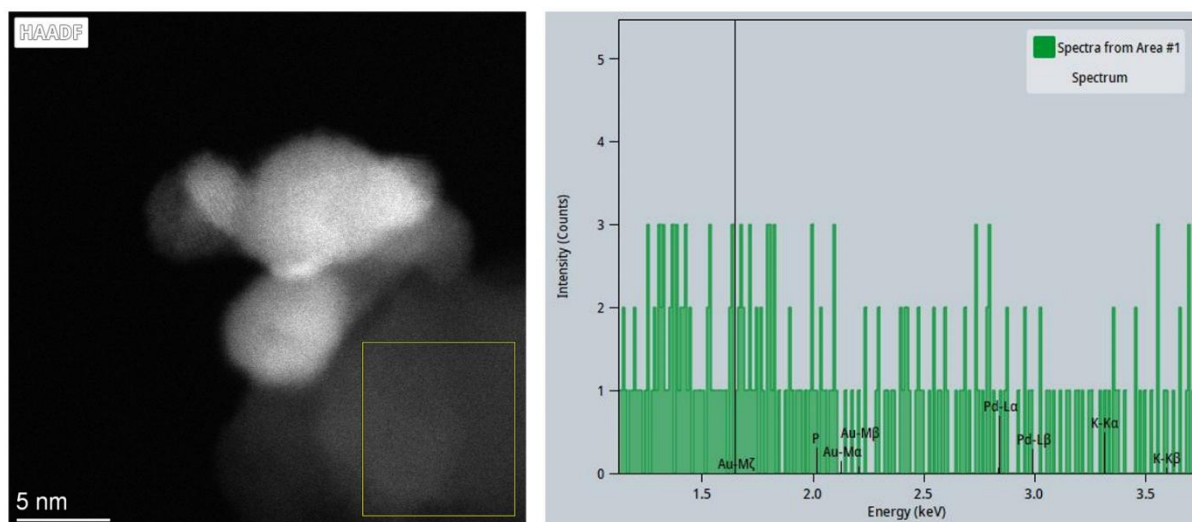
Figure S.26. HAADF AC-STEM image of the used 1% Au_1Pd_1/TiO_2 with X-EDS spot analysis revealing the absence of sub-nano (< 1 nm) monometallic Pd species on the support surface.
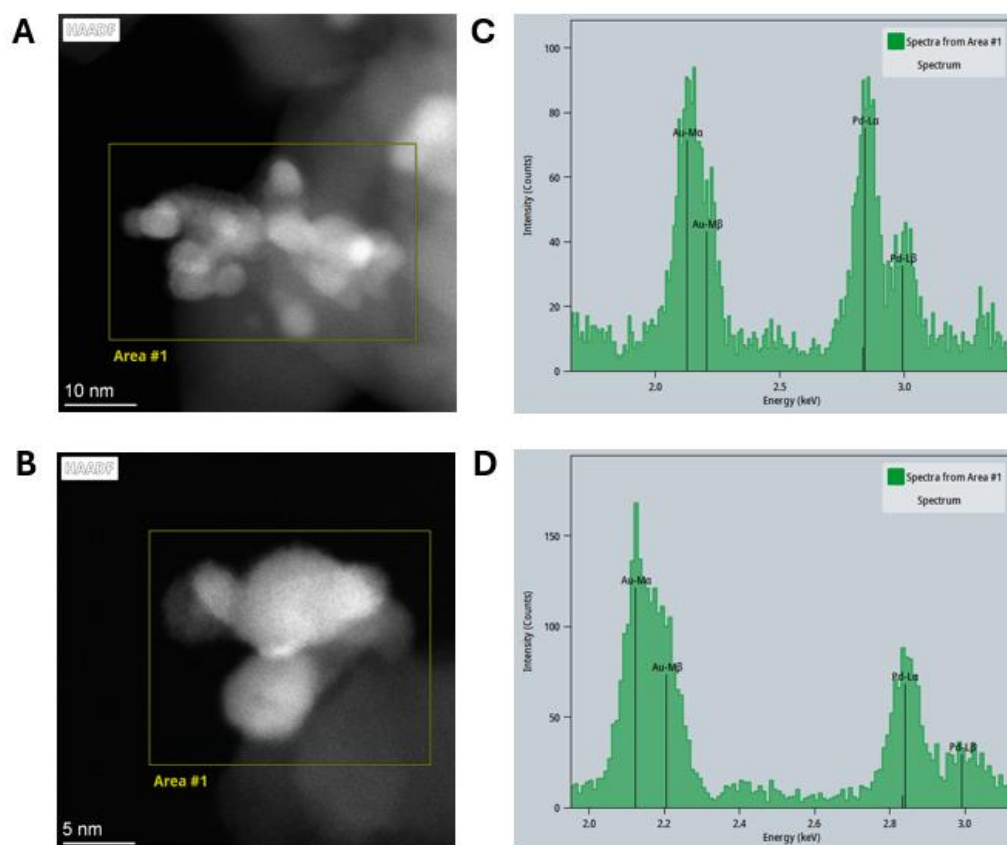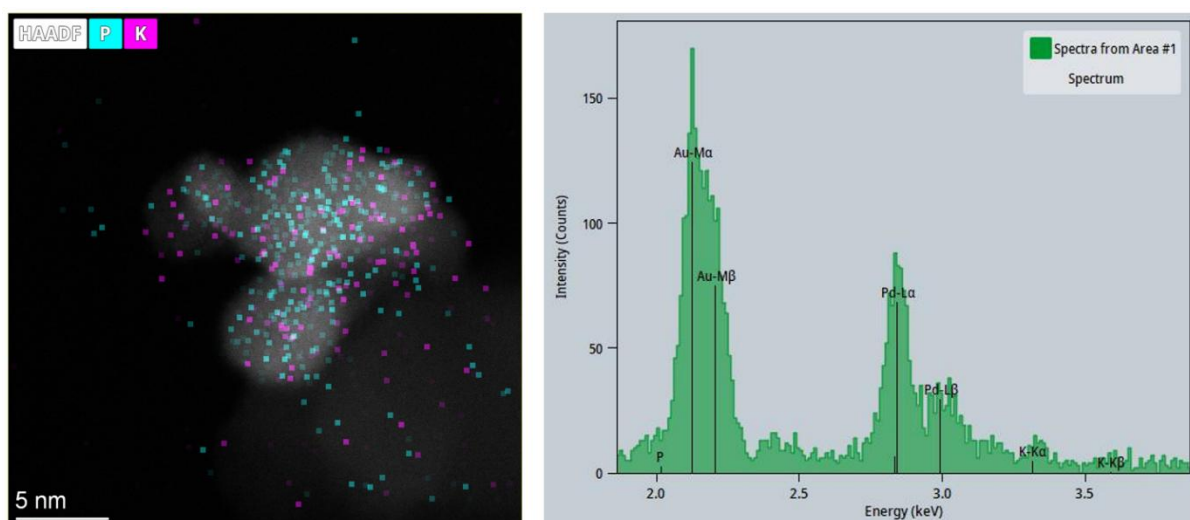
Figure S.27. HAADF AC-STEM image of the used 1% Au_1Pd_1/TiO_2 with X-EDS spot analysis revealing the presence of Pd and K species.
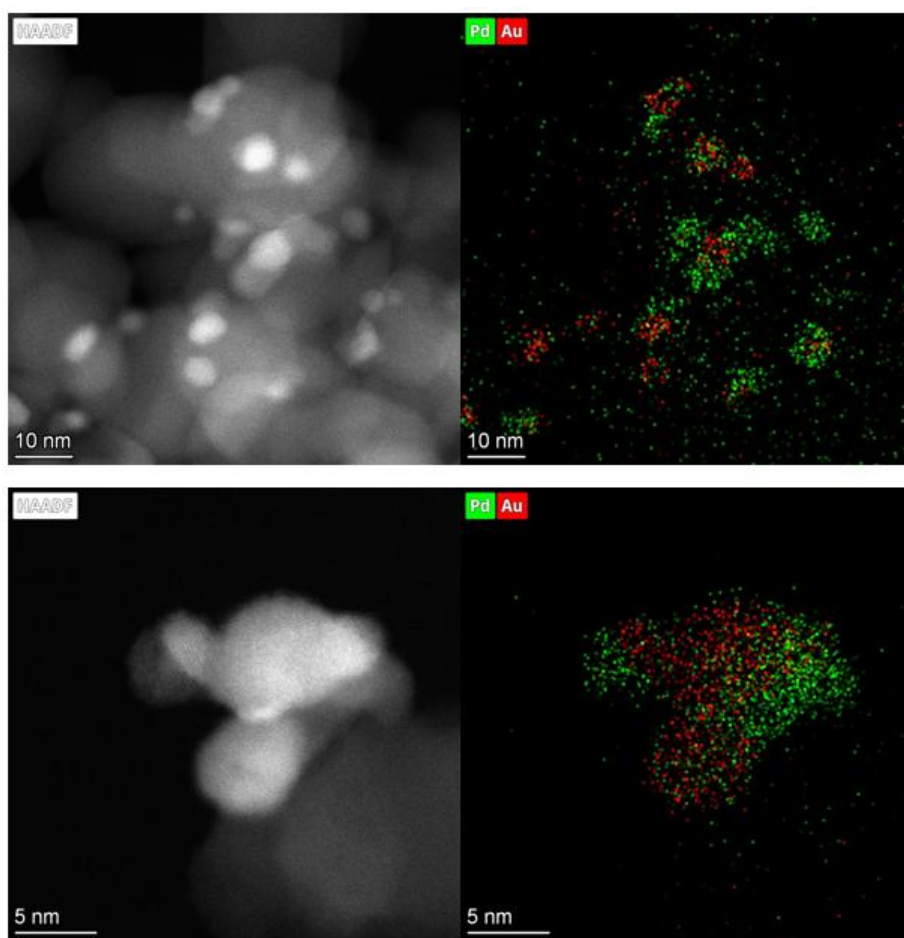
Figure S.28. HAADF AC-STEM X-EDS imaging of the used 1% Au_1Pd_1/TiO_2 catalyst following a model H_2O_2 synthesis reaction conditions over 2 h. **Model H_2O_2 direct synthesis reaction conditions:** catalyst (0.01 g), 2 bar (80% H_2 in air), potassium phosphate buffer (10 mM, pH 5.0, 10 mL) with 50 vol.% t-BuOH, 250 rpm, 20 °C, 2 h.
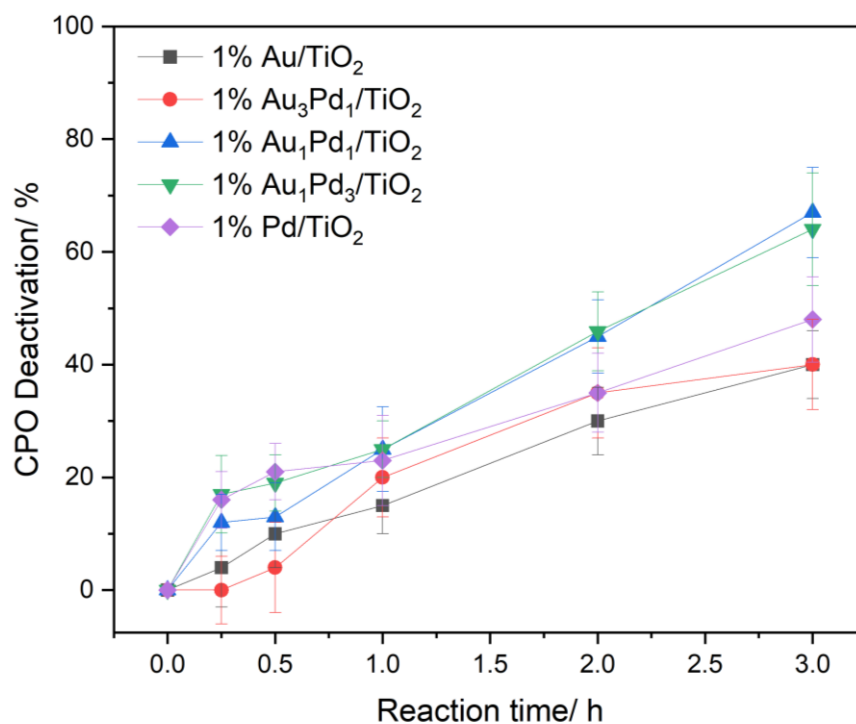
Figure S.29. Extent of CPO deactivation following chemo-enzymatic indole oxidation reactions with the 1%AuPd/TiO_2 catalysts, as determined *via* the MCD assay. **Indole oxidation reaction conditions:** catalyst (0.001 g), CPO (600 nM, 15 UmL^{-1}), indole (10 mM), potassium phosphate buffer (10 mM, pH 5.0, 10 mL) with 50 vol.% *t*-BuOH, 2 bar (80 % H_2 in air), 250 rpm, 20 °C, 0 – 2 h. **MCD assay reaction conditions:** post-reaction aliquot (100 μL), assay solution (900 μL, 0.1 mM MCD, 20 mM KCl, 100 mM pH 2.75 potassium phosphate buffer), absorbance monitored at 278 nm (ε_{278} = 12200 M^{-1}cm^{-1}), 25 °C.

Table S.9: Extent of CPO deactivation, as determined by the MCD assay, following exposure to chloride salt solution.

Metal salt	Model leaching/ %	Precious Metal Concentration/ M	Chloride concentration/ M	CPO deactivation/ %
1% Au$_1$Pd$_1$/TiO$_2$*	0.04	1.8×10^{-8}	-	2.3 ± 1.0
HAuCl$_4$	0.2	1.0×10^{-8}	3.8×10^{-8}	3.3 ± 0.8
	0.3	1.5×10^{-8}	5.7×10^{-8}	4.0 ± 1.2
	0.4	2.0×10^{-8}	7.5×10^{-8}	4.0 ± 1.1
PdCl$_2$	0.2	1.9×10^{-8}	4.1×10^{-8}	2.8 ± 0.7
	0.3	2.8×10^{-8}	6.1×10^{-8}	3.5 ± 0.9
	0.4	3.8×10^{-8}	8.1×10^{-8}	4.0 ± 1.3
NaCl	-	-	8.1×10^{-8}	2.8 ± 1.1
MgCl$_2$	-	-	8.1×10^{-8}	2.6 ± 0.8
None	-	-	-	2.5 ± 1.0

Model leaching reaction conditions: CPO (600 nM, 15 UmL^{-1}), chloride salts (1.0×10^{-8} M – 3.8×10^{-8} M), potassium phosphate buffer (10 mM, 10 mL, pH 5.0), ambient pressure, 250 rpm, 20 °C, 2 h. **MCD assay reaction conditions:** diluted post-reaction aliquot (100 µL), assay solution (900 µL, 0.1 mM MCD, 20 mM KCl in 100 mM, pH 2.75 potassium phosphate buffer), absorbance monitored at 278 nm (ε_{278} = 12200 M^{-1}cm^{-1}), 25 °C. **Chloride salts:** HAuCl$_4$ (1.0×10^{-8} – 2.0×10^{-8} M), PdCl$_2$ (1.9×10^{-8} – 3.8×10^{-8} M), NaCl (8.1×10^{-8}M), MgCl$_2$ (8.1×10^{-8} M). **Note:** *CPO exposed to metal species leached from 1%AuPd/TiO$_2$ following model H$_2$O$_2$ synthesis reaction, with metal concentration determined by ICP-MS (chloride salts not present).
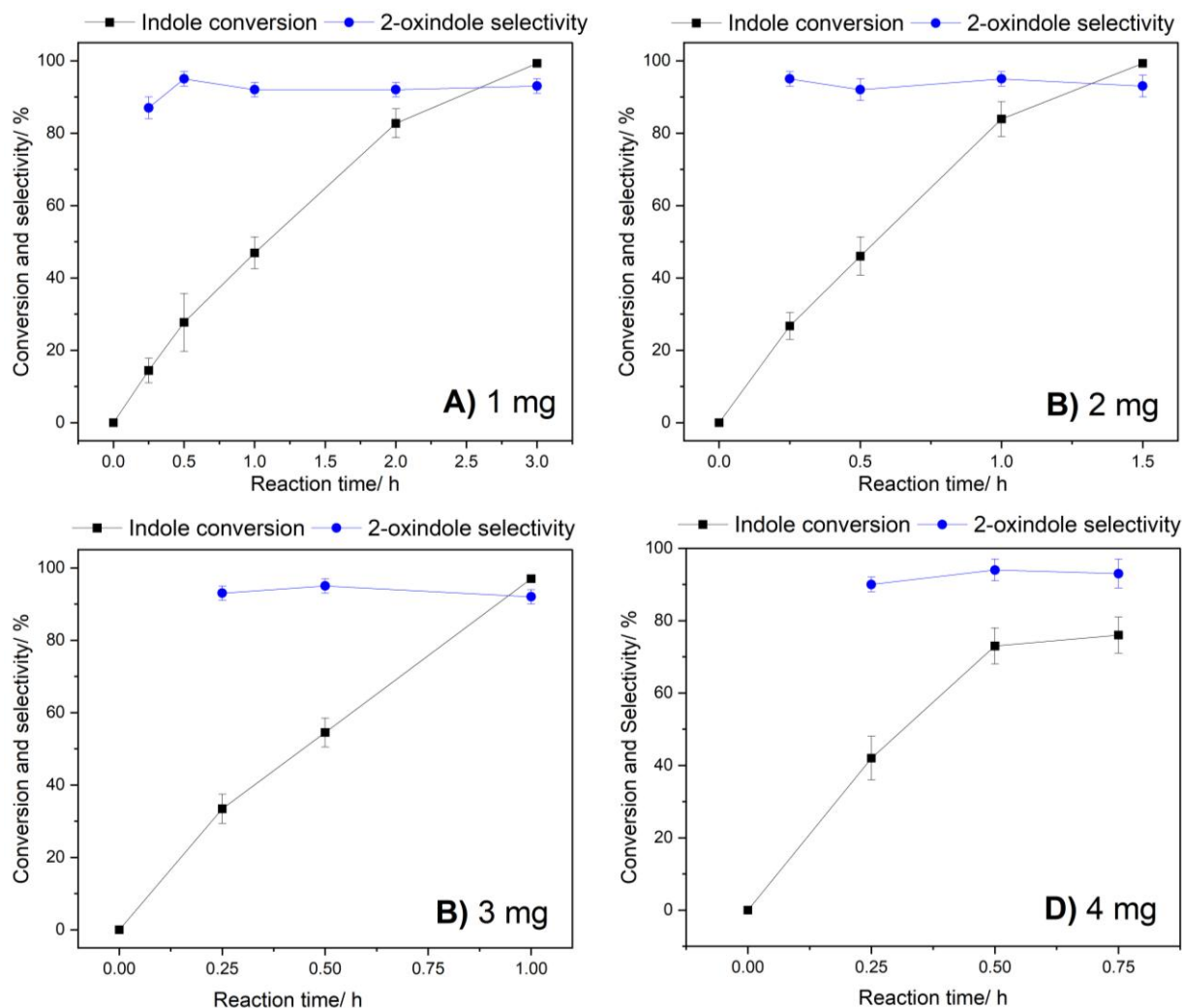
Figure S.30. Catalytic activity of 1%Au$_1$Pd$_1$/TiO$_2$ towards indole oxidation in the CPO chemo-enzymatic cascade, as a function of chemo-catalyst mass. **Indole oxidation reaction conditions:** 1%Au$_1$Pd$_1$/TiO$_2$ (0.001 − 0.004 g), CPO (600 nM, 15 UmL^{-1}), indole (10 mM), potassium phosphate buffer (10 mM, 10 mL, pH 5.0) with 50 vol.% *t*-BuOH, 2 bar (80 % H$_2$ in air), 250 rpm, 20 °C, 0 − 3 h. **Key: A)** 1 mg, **B)** 2 mg **C)** 3 mg **D)** 4 mg.
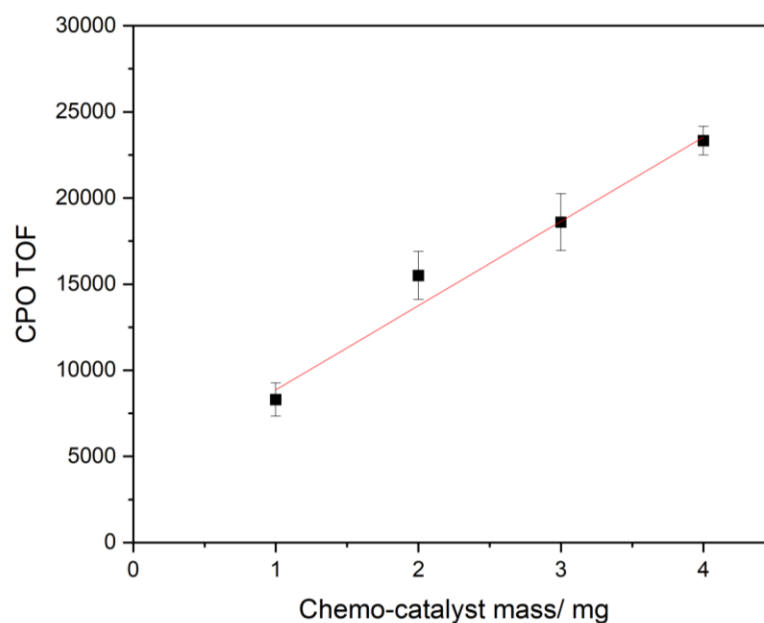
Figure S.31. Effect of chemo-catalyst mass on CPO TOF under chemo-enzymatic cascade conditions, as determined *via* 2-oxindole formation at 0.5 h. **Indole oxidation reaction conditions:** 1%Au_1Pd_1/TiO_2 (0.001 – 0.004 g), CPO (600 nM, 15 UmL^{-1}), indole (10 mM), potassium phosphate buffer (10 mM, 10 mL, pH 5.0) with 50 vol.% *t*-BuOH, 2 bar (80 % H_2 in air), 250 rpm, 20 °C, 0.5 h.

Figure S.32. Extent of CPO deactivation under chemo-enzymatic cascade reaction conditions in the absence and presence of indole, as determined *via* the MCD assay. **Indole oxidation reaction conditions:** catalyst (0.001 – 0.004 g), CPO (600 nM, 15 UmL^{-1}), indole (0 mM or 10 mM), potassium phosphate buffer (10 mM, 10 mL, pH 5.0) with 50 vol.% *t*-BuOH, 2 bar (80 % H$_2$ in air), 250 rpm, 20 °C, 0 – 3 h. **MCD assay reaction conditions:** dilu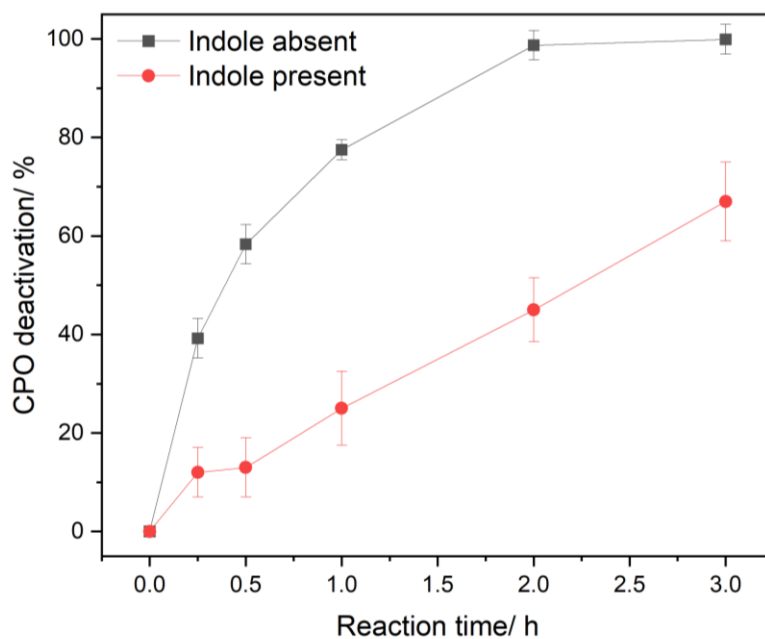ted post-reaction aliquot (100 µL), assay solution (900 µL, 0.1 mM MCD, 20 mM KCl in 100 mM, pH 2.75 potassium phosphate buffer), absorbance monitored at 278 nm (ε_{278} = 12200 M^{-1}cm^{-1}), 25 °C.
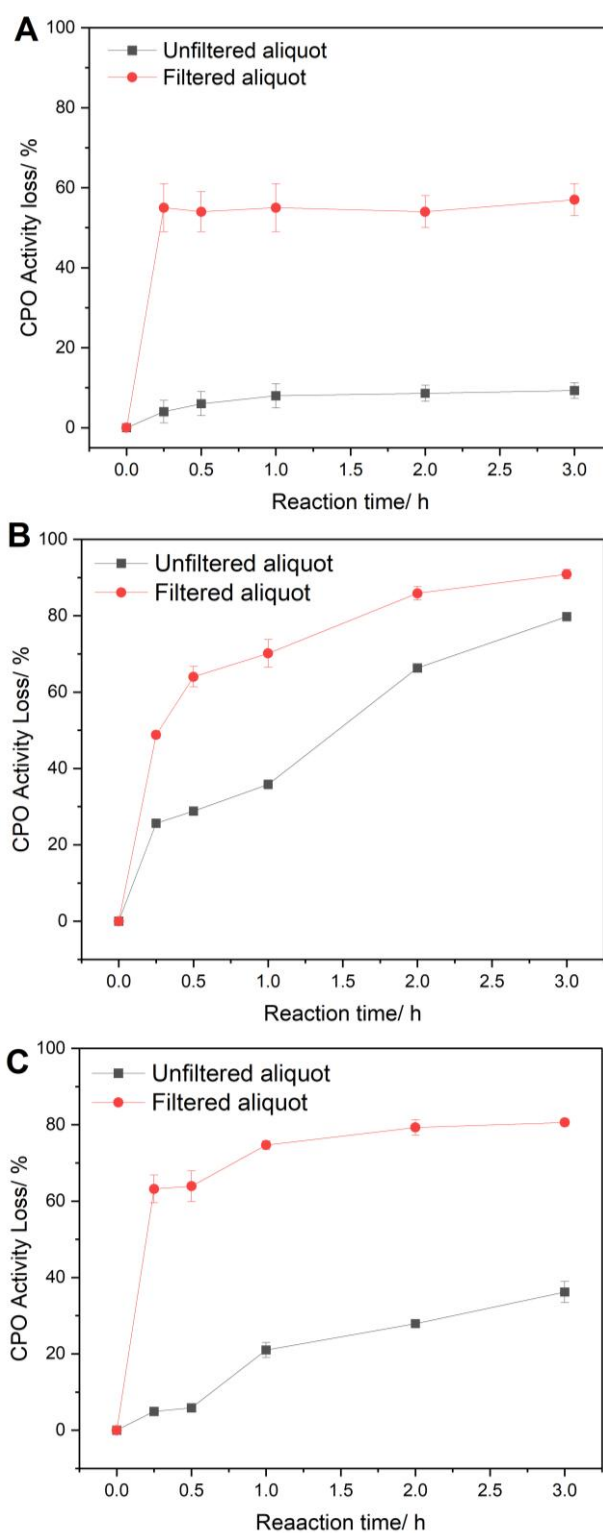
Figure S.33. Effect of reaction conditions on CPO activity in the presence of 1%Au$_1$Pd$_1$/TiO$_2$ and TiO$_2$, as determined by the MCD assay. **Reaction conditions:** catalyst (0.001 – 0.003 g) or TiO$_2$ (0.001 g), potassium phosphate buffer (10 mL, 10 mM, pH 5.0) with 50 vol.% *t*-BuOH, 2 bar (80 % N$_2$ in air), 20 °C, 250 rpm, 0 – 3 h. **MCD assay reaction conditions:** filtered or unfiltered aliquot (100 µL), assay solution (900 µL, 0.1 mM MCD, 20 mM KCl, 2 mM H$_2$O$_2$ in 100 mM, pH 2.75 potassium phosphate buffer), absorbance monitored at 278 nm (ε_{278} = 12200 M^{-1}cm^{-1}), 25 °C. **Key: A)** TiO$_2$ (0.001 g), **B)** 1%Au$_1$Pd$_1$/TiO$_2$ (0.001 g), **C)** 1%Au$_1$Pd$_1$/TiO$_2$ (0.003 g).
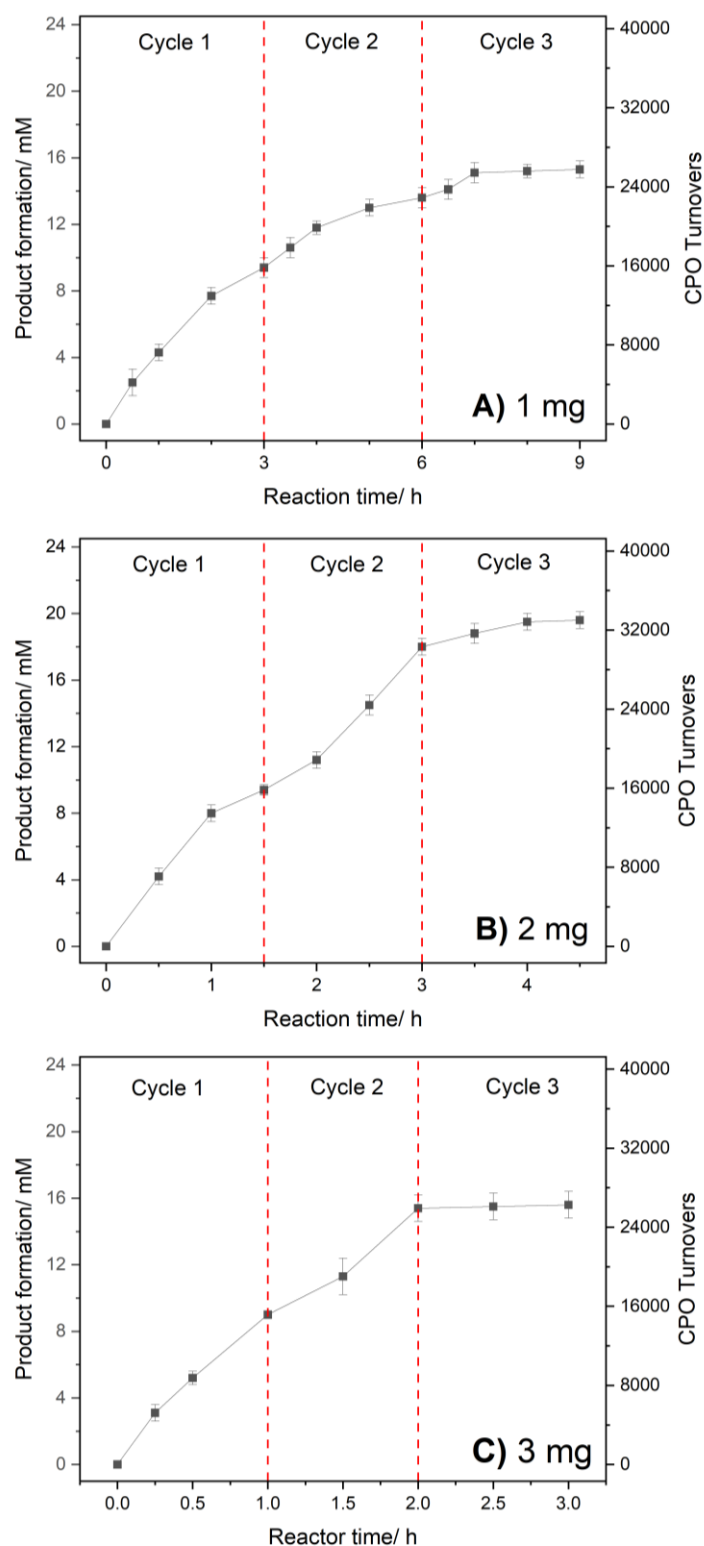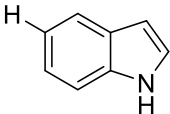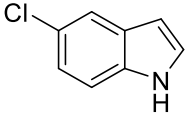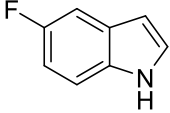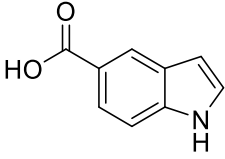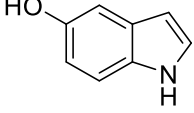
Figure S.34. Comparison of the chemo-enzymatic indole oxidation cascade lifetime as a function of chemo-catalyst mass, probed *via* substrate recharging experiments. **Indole oxidation reaction conditions:** $1\%Au_1Pd_1/TiO_2$ (0.001 − 0.003 g), potassium phosphate buffer (10 mL, 10 mM, pH 5.0) with 50 vol.% *t*-BuOH, 2 bar (80 % H_2 in air), 20 °C, 250 rpm, 0 – 3 h. **Key: A)** 0.001 g catalyst, 3.0 h re-charging intervals, **B)** 0.002 g catalyst, 1.5 h recharging intervals, **C)** 0.003 g catalyst, 1.0 h recharging intervals. **Note:** indole (10 mM) and reagents gases (2 bar 80% H_2 in air) re-charged at indicated intervals (dashed red lines).

Table S10. Comparison of CPO indole oxidation efficacy from the literature, as an effect of *in situ* H_2O_2 supply strategy.

Ref	*In situ* H_2O_2 Supply Strategy	Co-catalyst	By-product of H_2O_2 Generation	CPO TTN
1	Co-enzymatic	Glucose Oxidase	Gluconic acid	34,000
2	Electrochemical	Gas-diffusion electrode	H_2O	39,000
This work	Chemo-catalytic	1% Au_1Pd_1/TiO_2	H_2O	33,000

Reaction conditions: Ref 1: Immobilized CPO/GOx on polyurethane foam (40 mg), indole (75 µmol), glucose (15 mM) citrate buffer (5 mL, 100 mM, pH 5.0), stirred at room temperature in a sealed vial. **Ref 2:** gas-diffusion electrode (16.5 cm^2, 1.8 $mAcm^{-2}$), CPO (100 nM), indole (3.9 mM), citrate buffer (100 nM, pH 2.75), sodium chloride (10 mM). **This work:** 0.5%Au-0.5%Pd/TiO_2 (0.002 g), potassium phosphate buffer (10 mL, 10 mM, pH 5.0) with 50 vol.% *t*-BuOH, 2 bar (80 % H_2 in air), 20 °C, 250 rpm, 4 h. Reagent gases (2 bar, 80% H2 in air) and indole (10 mM) re-charged at 1.5 h and 3 h.

Table S.11. Effect of oxidant supply on the catalytic activity of CPO for selective oxidation of indole derivatives.

Substrate	Indole Conversion (Selectivity)/ %		
	1) CPO + AuPd	2) CPO + H_2O_2 (N_2)	3) AuPd-only
	83 ± 3 (92 ± 3)	14 ± 3 (94 ± 2)	0.0 ± 0.7
	55 ± 4 (99 ± 2)	2.2 ± 0.4 (94 ± 3)	0.0 ± 0.8
	61 ± 4 (86 ± 4)	2.5 ± 0.3 (96 ± 4)	0.0 ± 0.7
	24 ± 5 (9 ± 2)	1 ± 0.3 (95 ± 3)	0.0 ± 0.3
	32 ± 3 (82 ± 3)	12.3 (80 ± 4)	0.0 ± 0.4

Substituted indole oxidation reaction conditions: 1) 1%Au_1Pd_1/TiO_2 (0.001 g), CPO (600 nM, 15 UmL^{-1}), indole (10 mM), potassium phosphate buffer (10 mL, 10 mM, pH 5.0) with 50 vol.% *t*-BuOH, 2 bar (80 % H_2 in air), 20 °C, 250 rpm, 2 h. **2)** CPO (600 nM, 15 UmL^{-1}), H_2O_2 (100 ppm), indole (10 mM), potassium phosphate buffer (10 mL, 10 mM, pH 5.0) with 50 vol.% *t*-BuOH, 2 bar N_2, 20 °C, 250 rpm, 2 h. **3)** 1%Au_1Pd_1/TiO_2 (0.001 g), indole (10 mM), potassium phosphate buffer (10 mL, 10 mM, pH 5.0) with 50 vol.% *t*-BuOH, 2 bar (80 % H_2 in air), 20 °C, 250 rpm, 2 h.

Table S.12. Techno-economic analysis for chemo-catalytic in situ H_2O_2 supply for indole oxidation compared to co-enzymatic and continuous addition strategies.

Material	Material Cost per ton 2-oxindole/ USD		
	Chemo-catalytic	Co-enzymatic (GOx)	H_2O_2 Continuous Addition
1%Au_1Pd_1/TiO_2	5.980	-	-
	25% Efficiency	120	-
H_2	50% Efficiency	60	-
	100% Efficiency	30	-
Solvent	24,000	24,000	359,300
H_2O_2	-	-	407
Total cost/ USD	30,040	67,130	

Note: H_2 consumption has been calculated based on estimated H_2 utilization efficiencies with respect to 2-oxindole formation.

Table S.13. Techno-economic analysis for chemo-catalytic in-situ H_2O_2 generation using the 1wt.%Au_1Pd_1/TiO_2 catalyst for CPO indole oxidation reported in this work.

Material		Unit	USD/ Unit	Cost per ton 2-oxindole/ USD
Catalyst	Au	g	108.8	4,125
	Pd	g	37.8	1,433
	TiO_2	T	1,500	113
	H_2SO_4	T	85	13
	$NaBH_4$	kg	284	295
	PVA	T	3172	0.32
Total catalyst cost/ USD				5979
H₂ Usage	25% Efficiency			30
	50% Efficiency	Kg	2	60
	100% Efficiency			120
Solvent	K_2HPO_4	T	1,300	18.2
	KH_2PO_4	T	110	1156
	t-BuOH	T	84.62	22,779
Total solvent cost/ USD				23,954
Total cost (25% H₂ efficiency)/ USD				29,963
Total cost (50% H₂ efficiency)/ USD				29,993
Total cost (100% H₂ efficiency)/ USD				30,053

Table S.14. Techno-economic analysis for continuous addition of ex situ H_2O_2 for CPO indole oxidase reported in this work.

	Material	Unit	USD/ Unit	Cost per ton 2-oxindole/ USD
	Glucose oxidase	Kg	151	10,848
	Glucose	kg	0.5	32,329
	K_2HPO_4	T	1,300	18.2
Solvent	KH_2PO_4	T	110	1156
	t-BuOH	T	84.62	22,779
Total cost/ USD				67,130

Table S.15. Techno-economic analysis for continuous addition of ex situ H_2O_2 for CPO indole oxidase reported in this work.

	Material	Unit	USD/ Unit	Cost per ton 2-oxindole/ USD
	H_2O_2	T	797	407
	K_2HPO_4	T	1,300	273
Solvent	KH_2PO_4	T	110	17,350
	t-BuOH	T	84.62	341,700
Total cost/ USD				359,300

Table S.16. Comparison of E-factors for CPO indole oxidation with H_2O_2 supply *via* chemo-catalytic, co-enzymatic, or continuous addition strategies.

H₂O₂ Supply Strategy		Mass product/ g	Mass waste/ g	E-factor
Co-enzymatic		0.0028	9.06	3,250
Continuous addition		0.012	142.06	11,470
Chemo-catalytic	Single reaction cycle	0.013	8.88	670
	Substrate recharging	0.026	8.88	340

Continuous H₂O₂ addition reaction conditions: H_2O_2 reservoir (1.36 mM), pump (50 mL/h), CPO (15 UmL^{-1}, 600 nM), indole (10 mM), potassium phosphate buffer (10 mL, 10 mM, pH 5.0) with 50 vol.% *t*-BuOH, ambient pressure, 250 rpm, 20 °C, 0 – 3 h. **Co-enzymatic reaction conditions:** glucose oxidase (0.2 UmL^{-1}), glucose (100 mM), CPO (15 UmL^{-1}, 600 nM), indole (10 mM), potassium phosphate buffer (10 mL, 10 mM, pH 5.0) with 50 vol.% t-BuOH, ambient pressure, 250 rpm, 20 °C, 0 – 3 h. **Chemo-enzymatic reaction conditions:** 1%Au_1Pd_1 (0.001 g), CPO (15 UmL^{-1}, 600 nM), indole (10 mM), potassium phosphate buffer (10 mL, 10 mM, pH 5.0) with 50 vol.% t-BuOH, 2 bar (80% H_2 in air), ambient pressure, 250 rpm, 20 °C, 0 – 3 h. **Substrate recharging reaction conditions:** 1%Au_1Pd_1/TiO_2 (0.002 g), CPO (600 nM, 15 UmL^{-1}), indole (10 mM), potassium phosphate buffer (10 mL, 10 mM, pH 5.0) with 50 vol.% *t*-BuOH, 2 bar (80% H_2 in air), 20 °C, 250 rpm, 0 – 3 h, substrate recharging (indole and reagent gases) conducted at 1.5 h intervals.

Table S17. Specific surface measurements of 1wt.% AuPd/TiO2 catalyst series, as determined by BET.

Catalyst	Surface area / m^2g^{-1}
TiO_2 (P25)	60
1% Au/TiO_2	59
1%Au_3Pd_1/TiO_2	57
1%Au_1Pd_1/TiO_2	50
1%Au1Pd_3/TiO_2	50
1% Pd/TiO_2	55

Surface area measurements: N_2 employed as adsorbate using a 5-point isotherm at -196 °C. Samples were degassed at 250 °C for 2 h prior to analysis.
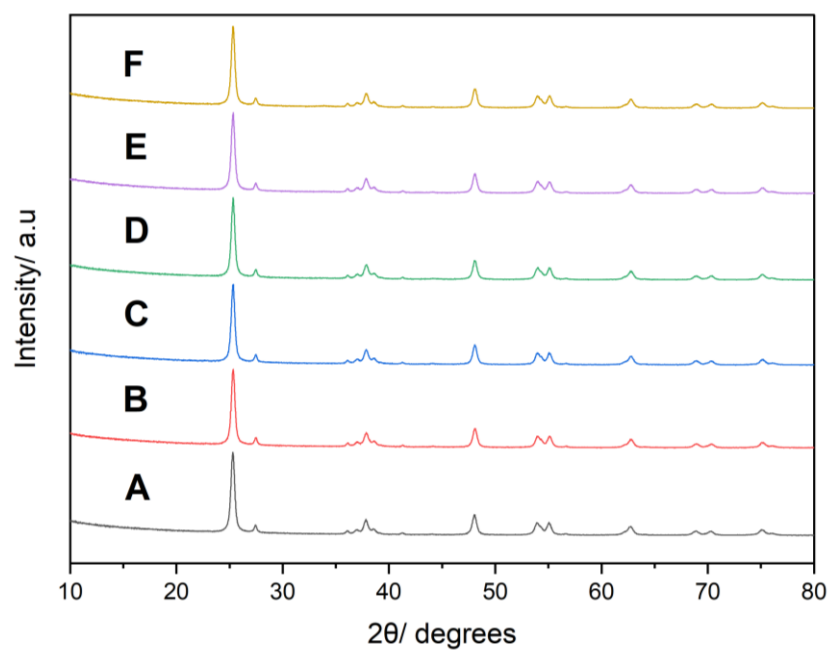
Figure S.35. X-ray diffractograms of 1wt.% AuPd/TiO$_2$ catalyst series. **A)** TiO$_2$ (P25), **B)** 1% Au/TiO$_2$, **C)** 1%Au$_3$Pd$_1$/TiO$_2$, **D)** 01%Au$_1$Pd$_1$/TiO$_2$, **E)** 1%Au$_1$Pd$_3$/TiO$_2$, and **F)** 1% Pd/TiO$_2$.

Experimental Methods

Catalyst Testing

Catalyst testing was conducted in sealed, gas tight 50 mL round bottom flasks rated to 60 psi and stirred using a Radley 6 Plus Carousel (0 – 1000 rpm) equipped with gas distribution system. The reactor is charged from a gas mixing tank, which is connected to H_2, N_2 and compressed air cylinders. The reactant gases are connected to the mixing tank on independent gas lines with corresponding pressure regulators, allowing the ratio of mixing gases to be controlled. The mixing tank is connected to the reactor with a pressure regulator allowing the reactor to be charged at controlled pressures. A schematic representation of the Radleys reactor setup is shown in Figure S36.
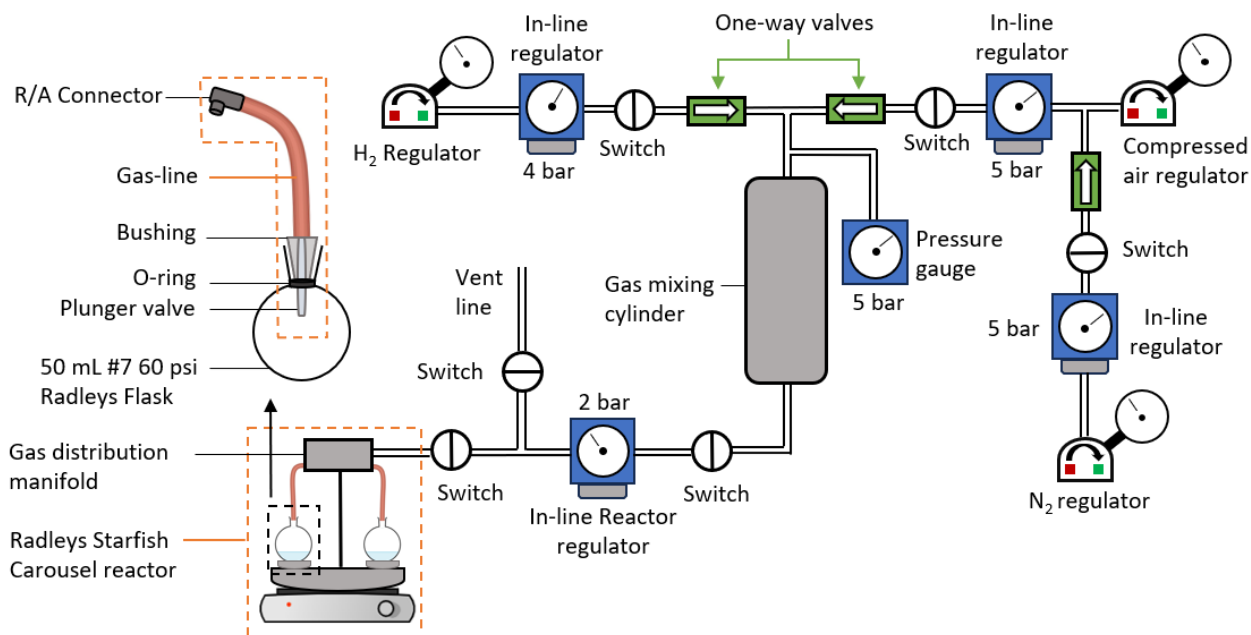

Figure S.36. Schematic representation of gas mixing and distribution setup for the Radleys carousel Starfish reactor used for catalyst testing, including the sealed Radleys glassware employed.

Model H$_2$O$_2$ Synthesis Reactions and Catalyst Reuse

Model H_2O_2 synthesis reactions were performed to generate used catalyst samples, which were subsequently utilized for chemo-enzymatic indole oxidation and H_2O_2 synthesis experiments, allowing catalyst reusability to be assessed. Model experiments were performed with ten-times the typical catalyst mass (0.01 g), allowing sufficient quantities of catalyst material to be generated for subsequent applications and analysis. The used catalyst was collected by vacuum filtration and washed reaction solvent before drying under vacuum (30 °C, 16 h). Aliquots of dried sample (0.001 g) were assessed for H_2O_2 direct synthesis or chemo-enzymatic cascade activity. Characterization (XPS, HAADF AC-STEM X-EDS, ICP-MS) of the used catalyst material was generated under the outlined model H_2O_2 synthesis reaction conditions.

Indole Oxidation with CPO and ex situ H$_2$O$_2$

Indole oxidation reactions with *ex situ* H_2O_2 (50 wt.%, stabilized, Merck) were performed using the low-pressure Radleys 6 Plus Carousel batch reactor. Indole (Merck) was dissolved in the reaction solvent (10 mL, 10 mM, pH 5.0 potassium phosphate buffer with 50 vol.% *t*-BuOH) to give the desired substrate

concentration (10 mM). Pre-formed H_2O_2 was subsequently charged in a single injection at concentrations comparable to that measured in chemo-catalytic H_2O_2 synthesis experiments (25 – 100 ppm), with an additional experiment performed at indole: H_2O_2 = 1: 1 (340 ppm, 10 mM H_2O_2). CPO (15 U mL$_{RM}^{-1}$, 600 nM) was charged before the glassware was sealed, purged and pressurized with N_2 (2 bar). The reactions were stirred (250 rpm) at ambient temperature (20 °C) for 2 h. Upon completion of a standard 2 hour reactions, filtered post-reaction aliquots were subjected HPLC analysis to determine product mixtures. Residual H_2O_2 concentration was determined using UV/vis spectroscopy on the aqueous layer following extraction of the organic products with ethyl acetate (2 x 10 mL).

Further experiments were conducted *via* the continuous addition of *ex situ* H_2O_2 from an external reservoir (1.36 mM) using a peristaltic pump (50 mL/h) and round-bottom flask (250 mL) reaction vessel. Indole was dissolved in reaction solution (10 mL, 10 mM, pH 5.0 potassium phosphate buffer with 50 vol.% *t*-BuOH) to give the desired substrate concentration (10 mM), before charging with CPO (15 UmL$_{RM}^{-1}$, 600 nM) and initiating the reaction with oxidant addition *via* the peristaltic pump. Reactions were stirred (250 rpm) at ambient temperature (20 °C) up to 3 h reaction time. Aliquots of reaction mixture (100 μL) sampled and filtered before subjecting to HPLC analysis to determine products mixtures.

Indole Oxidation with CPO and Glucose Oxidase (GOx)

To evaluate indole oxidation rates using H_2O_2 generated *in situ* by GOx, experiments were conducted in open-top round bottom flasks. Indole (10 mM) and glucose (100 mM) were dissolved in reaction mixture (10 mL, 10 mM, pH 5.0 potassium phosphate buffer with 50 vol.% *t*-BuOH) before charging with CPO (15 UmL$_{RM}^{-1}$, 600 nM) and GOx (0.2 UmL$_{RM}^{-1}$). Reaction mixtures with stirred (250 rpm) at ambient temperature (20 °C) for a given reaction time (15 – 180 min) before subjecting aliquots of post-reaction mixtures to HPLC analysis to determine product mixtures. One GOx activity unit is defined as 1.0 μmol of β-D-glucose converted to D-gluconolactone and H_2O_2 per minute at pH 5.1 at 35 °.

Chemo-catalytic Indole oxidation

Chemo-catalytic reactions were performed in the absence of CPO, allowing unselective pathways towards indole and 2-oxindole to be assessed. Indole (Merck) or 2-oxindole (Merck) was dissolved the reaction solvent (10 mL, 10 mM, pH 5.0 potassium phosphate buffer with 50 vol.% *t*-BuOH) to give the desired substate concentration (10 mM). The catalyst (0.001 g) was weighed directly into the 50 mL gas-tight round bottomed flasks, before addition of the reaction solvent and charging with reagent gases (2 bar, 80 % H_2 in air)*.* Additional experiments were conducted under a H_2-only environment (2 bar, 80% H_2 in N_2) to probe chemo-catalytic hydrogenation pathways. The reactions were stirred at 250 rpm at 20 °C for the over a standard 2 h reaction. Filtered post-reaction aliquots were subjected HPLC analysis to determine product mixtures. Residual H_2O_2 concentration was determined using UV/vis spectroscopy on the aqueous layer following extraction of the organic products with ethyl acetate (2 x 10 mL).

Enzymatic 2-oxindole Over-oxidation

Enzymatic contributions towards 2-oxindole over-oxindole were probed utilizing chemo-catalytically *in situ* generated H_2O_2 and pre-formed *ex situ* H_2O_2. 2-oxindole (Merck) was dissolved the reaction solvent (10 mL, 10 mM, pH 5.0 potassium phosphate buffer with 50 vol.% *t*-BuOH) to give the desired substate concentration (10 mM). For chemo-enzymatic experiments, the catalyst (0.001 g) was

weighed directly into the 50 mL gas-tight round bottomed flasks, before addition of the reaction solution and charging with reagent gases (2 bar, 80 % H_2 in air). For *ex situ* H_2O_2 experiments, the reaction vessel was charged with the reaction solution followed by pre-formed H_2O_2 (100 ppm) in a single injection, before charging with N_2 (2 bar). The reactions were stirred at 250 rpm at 20 °C for the over a standard 2 h reaction. Filtered post-reaction aliquots were subjected HPLC analysis to determine product mixtures. Residual H_2O_2 concentration was determined using UV/vis spectroscopy on the aqueous layer following extraction of the organic products with ethyl acetate (2 x 10 mL).

HPLC Calibration for Indole and 2-oxindole Quantification
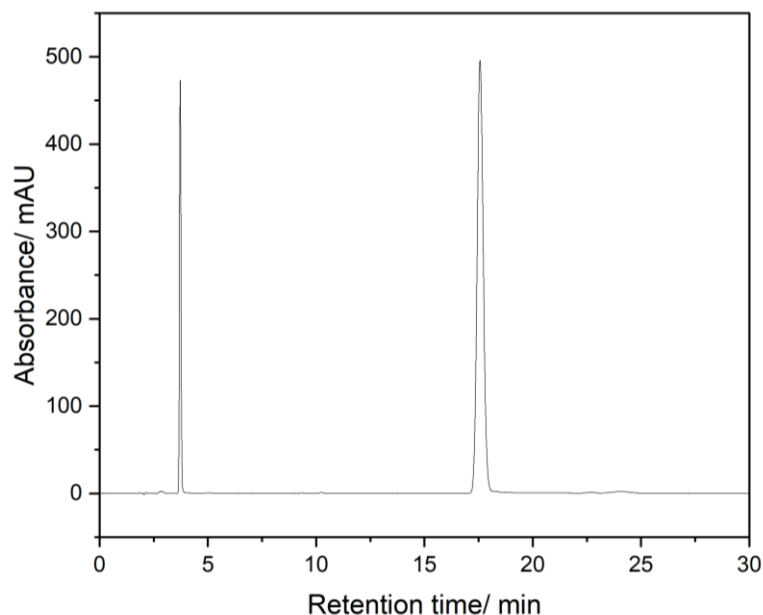
Figure S.37. Example HPLC chromatogram for post-reaction mixture following chemo-enzymatic indole oxidation reaction. **Retention times:** 2-oxindole (3.7 min), indole (17.5 min). **Method details:** Agilent 1200 series equipped with an Agilent Poroshell 120 EC-C18 (2.7 μm 4.6 x 150 mm) column and Agilent 1260 series DAD detector. Mobile phase of water/acetonitrile mixture (0.75 mLmin^{-1}, 70:30 with gradient elution to 50:50), column temperature maintained at 30 °C, eluants monitored at 278 nm.
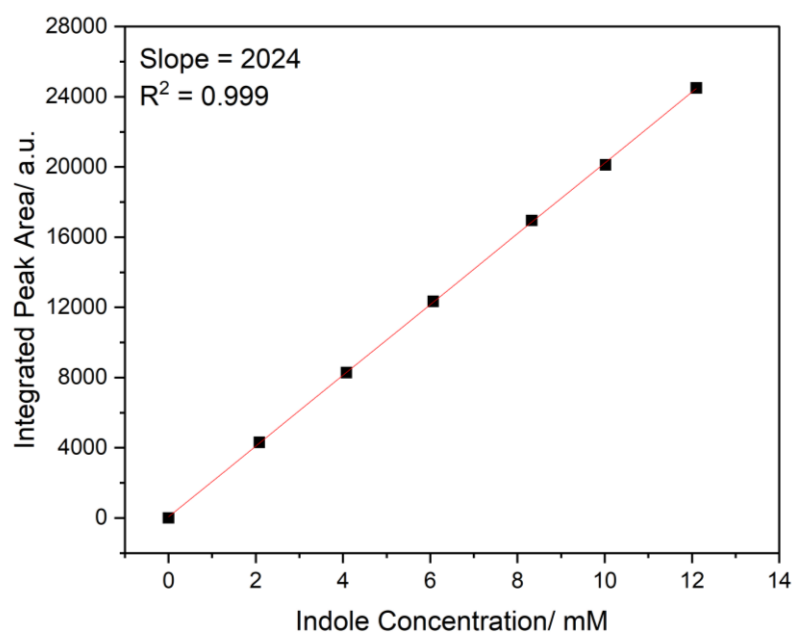
Figure S.38. HPLC calibration for indole in potassium phosphate buffer (10 mL, 10 mM, pH 5.0) with 50 vol.% *t*-BuOH. Agilent 1200 series equipped with an Agilent Poroshell 120 EC-C18 (2.7 μm 4.6 x 150 mm) column and Agilent 1260 series DAD detector. Mobile phase of water/acetonitrile mixture (0.75 mLmin^{-1}, 70:30 with gradient elution to 50:50), column temperature maintained at 30 °C, eluants monitored at 278 nm.

Figure S.39. HPLC calibration for 2-oxindole in potassium phosphate buffer (10 mL, 10 mM, pH 5.0) with 50 vol.% *t*-BuOH. Agilent 1200 series equipped with an Agilent Poroshell 120 EC-C18 (2.7 μm 4.6 x 150 mm) column and Agilent 1260 series DAD detector. Mobile phase of water/acetonitrile mixture (0.75 mLmin⁻¹, 70:30 with gradient elution to 50:50), column temperature maintained at 30 °C, eluants monitored at 278 nm.
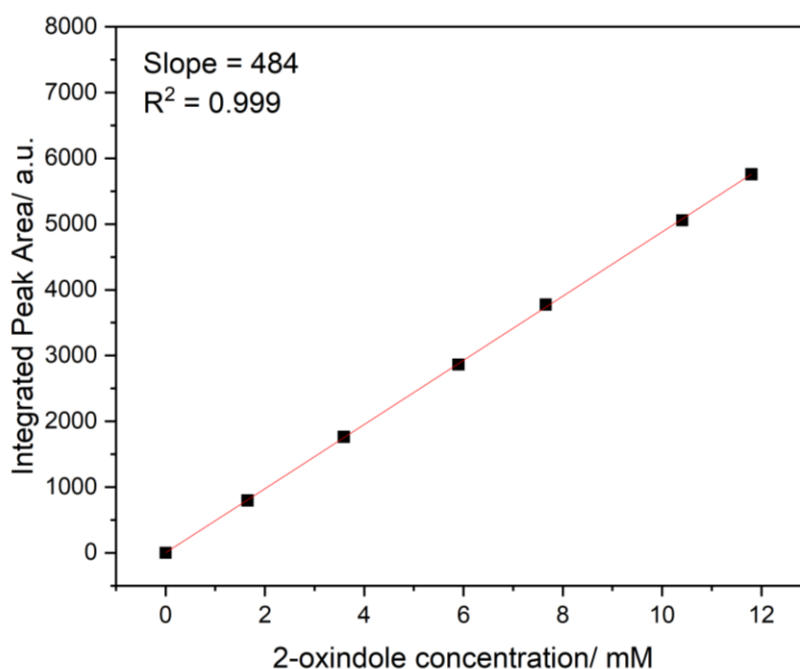
Determining CPO Deactivation Following Indole Oxidation Experiments

Upon completion of a reaction, unfiltered post-reaction aliquots (100 μL) were diluted in potassium phosphate buffer (900 μL, 10 mM, pH 5.0), before subjecting to to the monochlorodimedone (MCD) assay, according to the following established procedure.[5] Diluted CPO solution (100 μL) was added to the MCD assay reaction mixture (900 μL, 100 mM potassium phosphate buffer, pH 2.75, 0.1 mM MCD, 20 mM KCl, 2 mM H_2O_2) and substrate conversion was followed by measuring the absorbance of MCD at 278 nm (ε_{278} = 12200 M^{-1} cm^{-1}) at 25 °C using a Shimadzu UV/vis 1900i spectrophotometer. The CPO concentration was appropriately diluted to give linear enzyme kinetics. One activity unit (1 U) is defined as 1 μmol MCD converted in 1 min. To account for the inhibition of CPO activity assays by the product distribution present in post-reaction aliquots, the residual CPO activity was compared against a suitable assay inhibition model. This model was generated by preparing a series of model post reaction mixtures (0 - 10 mM indole, 0 – 10 mM 2-oxindole, 0, 25, 50, 75, 100% model indole conversions, e.g. 50% conversion contained 5 mM indole and 5 mM 2-oxindole) containing CPO (600 nM, 15 UmL⁻¹) in the reaction media employed for indole oxidation reactions (10 mL, 10 mM, pH 5.0 potassium phosphate buffer with 50 vol.% *t*-BuOH). CPO activity of the model post-reaction solutions was determined by the MCD assay and compared to the measured CPO activity observed in the absence of indole and 2-oxindole, allowing the extent of assay inhibition to be determined as a function of model indole conversion. The developed assay inhibition model was subsequently applied to post-reaction CPO activity assays, allowing the extent of CPO deactivation to be determined, as outlined below.
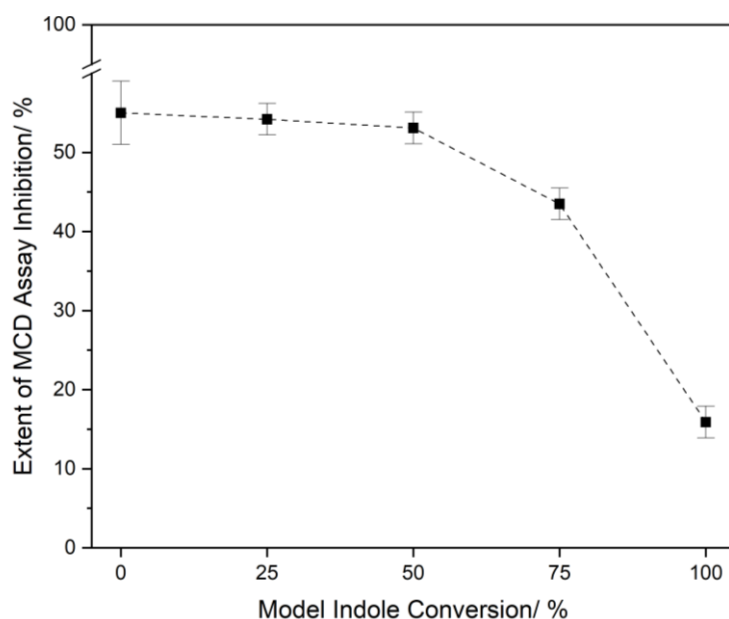
Figure S.40. Assay inhibition model showing the effect of indole and 2-oxindole on the standard MCD assay to determine CPO activity, as a function of model indole conversion. **Model post-reaction mixtures:** CPO (15 UmL^{-1}, 600 nM), indole (0 – 10 mM), 2-oxindole (0 – 10 mM), potassium phosphate buffer (10 mM, 10 mL, pH 5.0) with 50 vol.% t-BuOH. **MCD assay reaction conditions:** CPO solution (100 µL), assay solution (900 µL, 0.1 mM MCD, 20 mM KCl, 2 mM H$_2$O$_2$, 100 mM pH 2.75 potassium phosphate buffer), absorbance monitored at 278 nm (ε_{278} = 12200 M^{-1}cm^{-1}), 25 °C. Note: CPO in potassium phosphate buffer (100 mM, pH 2.75) prior to assay to give linear enzyme kinetics. **Note 1:** indole/2-oxindole concentrations in model post-reaction mixtures concentrations shown in Table S13. **Note 2:** Extent of inhibition determined by comparing measured CPO activity in the presence and absence of indole/2-oxindole.

Table S.18. The extent of MCD assay inhibition upon determining CPO activity, as a function of model indole oxidation conversion.

Model Indole Conversion/ %	Indole concentration/ mM	2-oxindole concentration/ mM	Extent of MCD Assay Inhibition/ %
0	10	0.0	55 ± 4
25	7.5	2.5	54.2 ± 2
50	5.0	5.0	53.1 ± 2
75	2.5	7.5	43.5 ± 2
100	0.0	10.0	15.9 ± 2

Table S.19. Linear segmentation of the MCD assay inhibition model shown in Figure S37, allowing the extent of assay inhibition to be determined as a function of indole conversion.

Model Conversion	Linear Functions		
Region/ %	Average	Upper	Lower
0 – 25	Y = 0.033x + 55.0	Y = -0.04x + 57.4	Y = -0.26x + 52.6
25 – 50	Y = -0.046x + 55.3	Y = -0.057x + 57.8	Y = 0.030x + 52.7
50 – 75	Y = -0.38x + 72.2	Y = -0.39x + 74.4	Y = -0.38x + 70.0
75 – 100	Y = -1.11x + 126.5	Y = -1.14x + 130.5	Y = -1.11x + 122.4

A linear segmentation method has been applied to the assay inhibition model, as shown in Table S13. This allowed the extent of inhibition (I) to be modelled as a function of indole conversion. This was subsequently applied to experimentally measured post-reaction activity (PRA), allowing the modelled PRA to be determined, as shown below:

$$\text{Modelled PRA} = \text{measured PRA} \times \frac{100}{100 - I}$$

The extent of CPO deactivation can then be determined by comparing the modelled PRA to the pre-reaction activity (PrRA).

$$\text{CPO deactivation (\%)} = 100 - \left[\left(\frac{\text{Modelled PRA}}{\text{PrRA}} \right) \times 100 \right]$$

To account for experimental error in assay inhibition model, this calculation is repeated at the upper and lower limits of the assay inhibition model. This is combined with the errors associated with the measured CPO activity and indole conversion, allowing an overall error to be calculated for the extent of CPO deactivation.

Techno-economic analysis and Determination of E-factor

Techno-economic analysis was conducted for each of H_2O_2 delivery systems investigated (chemo-catalytic, co-enzymatic, and continuous H_2O_2), which determined material cost in USD per ton 2-oxindole formation. Such calculations were based on the product formation following a 3 h reaction, wherein catalysis reached extinction (continuous addition and co-enzymatic) or complete substrate conversion (chemo-catalytic) was achieved, which is considered one reaction cycle. Based on this, the number of reaction cycles to obtain 1 ton product was calculated for each of the systems. Upon determining the cost of material to conduct one reaction, the cost of producing 1 ton of product could be calculated based the determined number of reactions required for achieve this. In the case of the chemo-catalytic system, three calculations were performed based on estimated H_2 utilization efficiencies, *i.e.* at 50% H_2 utilization efficiency the molar ratio of product formation: H_2 consumed is 1: 2.

To determine E-factors (mass waste/ mass product) for each of the H_2O_2 supply systems, numerous assumptions were employed. The mass of 2-oxindole was defined as the sole contributor to product mass. The mass of solvent (H_2O, *t*-BuOH, KH_2PO_4/K_2HPO_4) was determined for each of the systems and defined as waste. In the chemo-catalytic system, the mass of chemo-catalyst was not included in the mass of waste calculation, as precious metals from spent catalyst material can be recovered. Similarly,

the contribution of reagent gases was not considered, as these reagents can be easily recycled. CPO was not considered in any of the calculations, owing to its negligible and equal contribution to each of the systems. For the co-enzymatic approach, the mass of glucose was approximated to the mass of co-substrate/product waste, owing to the 1: 1 molar ratio of glucose and gluconic acid upon H_2O_2 production.

Catalyst Characterization

Inductively Coupled Plasma Mass Spectrometry ICP-MS

The extent of metal leaching was assessed *via* inductively coupled plasma mass spectrometry (ICP-MS) of post-reaction mixtures, using an Agilent 7900 ICP-MS equipped with I-AS auto-sampler. All samples were diluted by a factor of 10 using HPLC grade H_2O (1 % HNO_3 and 0.5% HCl matrix). All calibrants were matrix matched and measured against a five-point calibration using certified reference materials purchased from Perkin Elmer and certified internal standards acquired from Agilent. Importantly, model reactions were performed with 0.01 g of metal catalyst (ten times that utilized for a standard H_2O_2 direct synthesis experiment) in the absence of CPO or indole, allowing accurate determination of leached metal species by ICP-MS.

X-ray Photoelectron Spectroscopy (XPS)

X-ray photoelectron spectroscopy (XPS) measurements were performed on a Kratos Axis Ultra-DLD photoelectron spectrometer utilizing a monochromatic Al Kα X-ray source operating at 144 W(12 mA × 12 kV). Samples were pressed onto silicone-free double-sized Scotch tape and analysed using the hybrid spectroscopy mode, giving an analysis area of ca. 700 × 300 microns. High-resolution and survey spectra were acquired at pass energies of 40 eV (step size 0.1 eV) and 160 eV (step size 1 eV), respectively. Charge compensation was performed using low-energy electrons, and the resulting spectrum was calibrated to the lowest C(1s) peak from the fitted carbon core-level spectra, taken to be 284.8 eV. The suitability of the C(1s) referencing was confirmed by a secondary reference point, taken to be the Ti(2p3/2) peak with a binding energy of 458.7 eV, characteristic of that for virgin TiO_2. All data were processed using CasaXPS v2.3.24 using a Shirley background and modified Wagner factors as supplied by the instrument manufacturer. Peak fits were performed using a combination of Voigt-type functions (LA line shape in CasaXPS) and models derived from bulk reference samples where appropriate. The bulk structure of the catalysts was determined by powder X-ray diffraction using a (θ–θ) PANalytical X'pert Pro powder diffractometer using a Cu Kα radiation source, operating at 40 keV and 40 mA. Analysis was carried out using between 2θ values of 20°–80°.

Aberration Correction-Scanning Transmission Electron Microscopy (AC-STEM)

Aberration-corrected scanning transmission electron microscopy (AC-STEM) was performed using a probe-corrected ThermoFisherSpectra 200 S/TEM operating at 200 kV and a convergence semi-angle of 29.5 mrad. High spatial resolution STEM imaging wasacquired with a high-angle annular dark field (HAADF) detectoran inner collection angle of approximately 56 mrad (outer angleof approximately 200 mrad). Energy dispersive X-ray spectroscopy(EDX) was performed using a ThermoFisher Super-X detector, andthe data was analyzed using Thermo Scientific Velox Software.

Powder X-ray Diffraction (XRD)

X-ray diffraction of powder catalyst samples was conducting using a (θ-θ) PANalytical X'pert Pro powder diffractometer using a Cu Kα radiation source, operating a 40 KeV and 40 mA. Analysis was performed over a 40-minute run with a back-filled sample over 2θ of 10 − 80°.

Brunauer Emmett Teller (BET) Surface Area Measurements

BET surface area measurements were performed using a Quadrasorb surface area analyser. A 5-point isotherm of each material was measured using N_2 as absorbate gas. Samples were degassed at 250 ^{o}C for 2 h prior to surface area determination by 5-point N_2 adsorption at $-$ 196 ^{o}C, and data analysed using the BET method.

References

(1) van de Velde, F.; Lourenço, N. D.; Bakker, M.; van Rantwijk, F.; Sheldon, R. A. Improved operational stability of peroxidases by coimmobilization with glucose oxidase. *Biotechnol. Bioeng.* **2000**, *69* (3), 286-291.
(2) Krieg, T.; Hüttmann, S.; Mangold, K.-M.; Schrader, J.; Holtmann, D. Gas diffusion electrode as novel reaction system for an electro-enzymatic process with chloroperoxidase. *Green Chem.* **2011**, *13* (10), 2686-2689.